# Pure recoil corrections to the Lamb shift in hydrogenic atoms

M. Doncheski and H. Grotch
*Department of Physics, Pennsylvania State University, University Park, Pennsylvania 16802*

G. W. Erickson
*Department of Physics, University of California at Davis, Davis, California 95616*
(Received 17 September 1990)

The recoil corrections of order $(Z\alpha)^6 m^2/M$ to the hydrogenic Lamb shift are reviewed, and additional terms previously thought to be small are calculated numerically. It is found that significant contributions arise from single-transverse–single-Coulomb interactions in which the bulk of the contribution comes from negative-energy electron intermediate states. This term is found to contain a $\ln Z\alpha$ dependence, which accounts for its large effect. Other smaller terms are also computed and combined with all previous Lamb-shift contributions. The current status of the Lamb shift in hydrogen is reviewed.

## I. INTRODUCTION

In a recent series of papers the pure recoil corrections to the hydrogenic Lamb shift were studied in an attempt to obtain results to a level of precision of about 1 kHz. The present paper provides a more complete version of the previous work, a detailed presentation of the methodology utilized, and a calculation of new "large" corrections originally believed to be negligible.

Section II contains a discussion of the approach to the hydrogenic bound-state problem, including recoil. This proceeds from a three-dimensional two-body formalism in which the more massive particle is on its positive-energy mass shell. In Sec. III a review of the leading recoil corrections is presented, while in Sec. IV we present recently published higher-order contributions, and also estimate the recoil effects which would result from contributions not contained in the finite-proton-radius results. In Sec. V new higher-order effects are examined and calculated, and numerical results are given for the hydrogen atom. Finally, a review of Lamb-shift results is presented in Sec. VI, the conclusion.

## II. REVIEW OF A THREE-DIMENSIONAL BOUND-STATE FORMALISM

The calculation of hydrogenic energy levels for a Dirac electron interacting with an infinitely massive proton, namely the Dirac-Coulomb problem, was solved a longtime ago. However, when the proton is treated with finite mass $M$, an exact solution is no longer accessible since there are an infinite number of irreducible Feynman diagrams which contribute to the interaction kernel. This circumstance prevails in either a Bethe-Salpeter formalism or in one of the many possible three-dimensional bound-state approaches in use. Thus a truncation of kernels is necessary and only those kernels which contribute to a given order in the expansion parameters are needed. The relevant parameters are $Z\alpha$ and $m/M$. Moreover, except for factors of reduced mass, the second parameter will only be retained linearly, that is, higher powers of $m/M$ will not be necessary. In view of this it suffices to treat the nucleus (e.g., proton) from the very beginning as a nonrelativistic particle. Since our primary interest in this work is in effects which are independent of nuclear spin, we shall assume a spinless nucleus.

To formulate the bound-state problem we utilize an approach of Gorelick and Grotch[1] and specialize at the very beginning to a nonrelativistic nucleus. The exact four-dimensional equation for the four-point function of two fermions (without radiative corrections) is

$$K_P(p',p)-K_P^0(p',p)=\frac{i}{\not p_3-m+i\epsilon}\frac{i}{\not p_4-M+i\epsilon}\left[G(p',p)\frac{i}{\not p_1-m+i\epsilon}\frac{i}{\not p_2-M+i\epsilon}+\int d^4q\frac{1}{(2\pi)^4}G(p',q)[K_P(q,p)-K_P^0(q,p)]\right]. \tag{2.1}$$

This equation contains all Feynman diagrams except for the radiative corrections, which, if needed, can be separately calculated. We have mentioned that one of the particles is nonrelativistic and spinless. The corresponding equation for this case is

 

$$K_P(p',p)-K_P^0(p',p)=\frac{i}{\not p_3-m+i\epsilon}\frac{i}{p_{40}-\mathbf{p}_4^2/2M+i\epsilon}\left[G(p',p)\frac{i}{\not p_2-m+i\epsilon}\frac{i}{p_{20}-\mathbf{p}_2^2/2M+i\epsilon}\right.$$
$$\left.+\int d^4q\frac{1}{(2\pi)^4}G(p',q)[K_P(q,p)-K_P^0(q,p)]\right] . \tag{2.2}$$

In this expression the irreducible Feynman diagrams are those of a relativistic electron interacting with a nonrelativistic spinless proton. In the Coulomb gauge the lowest-order contributions to $G$ come from single-Coulomb and single-convection interactions. In the next order we have double-Coulomb, Coulomb-convection, convection-convection, and seagull contributions. Special care must be taken to include only irreducible contributions. One of the major difficulties of calculating bound-state energies manifests itself in the necessity to include in $G$ contributions from infinite-order perturbation theory. We will return to this point in detail later and show that other methods can be successfully applied in this instance.

In the preceding equations, we write each of the momenta in terms of relative and center-of-mass momenta

$$p_1=p+\mu_1P,\quad p_2=-p+\mu_2P ,$$
$$p_3=p'+\mu_1P,\quad p_4=-p'+\mu_2P ,$$

where $\mu_1=m/(m+M)$ and $\mu_2=M/(m+M)$. The function $K_P-K_P^0$ has a pole as $P_0$ approaches bound-state energies $E=m+M+\epsilon$. By means of appropriate definitions we introduce corresponding functions in the neighborhood of the poles. Let

$$\tilde{K}_{Pb}(\mathbf{p}',\mathbf{p})=\lim_{\substack{p_0'\to\mu_2\epsilon-\mathbf{p}'^2/2M\\ p_0\to\mu_2\epsilon-\mathbf{p}^2/2M}}\left[-p_0'+\mu_2\epsilon-\frac{\mathbf{p}'^2}{2M}\right]\left[-p_0+\mu_2\epsilon-\frac{\mathbf{p}^2}{2M}\right][K_{Pb}(p',p)-K_{Pb}^0(p',p)] . \tag{2.3}$$

This defines a function when the massive particle goes on shell and consequently the residue at the poles of $p_0$ and $p_0'$ is fixed by the preceding mass-shell constraint. In the vicinity of a bound-state pole $M_b$ the function $\tilde{K}_{Pb}(\mathbf{p}',\mathbf{p})$ will have a simple pole at $P_0=M_b$ with a residue at the pole which is proportional to the product of functions $f_{Pb}(\mathbf{p}')\bar{f}_{Pb}(\mathbf{p}')$, each of which is proportional to a wave function. Through this procedure we arrive at a three-dimensional equation

$$\psi_{P\alpha}(\mathbf{p}',s')=\frac{1}{\not p_3-m+i\epsilon}\sum_{s''}\int d^3q\frac{1}{(2\pi)^3}V_{\text{eff}}(\mathbf{p}',\mathbf{q},s',s'')\psi_{P\alpha}(\mathbf{q},s'') , \tag{2.4}$$

where $V_{\text{eff}}$ is an effective potential whose construction we now proceed to discuss.

We write several expressions for $\tilde{K}_{Pb}(\mathbf{p}',\mathbf{p})$. The first is

$$\tilde{K}_{Pb}(\mathbf{p}',\mathbf{p})=\frac{1}{\not p_3-m+i\epsilon}G(\mathbf{p}',\mathbf{p})\frac{1}{\not p_1-m+i\epsilon}$$
$$+\frac{1}{\not p_3-m+i\epsilon}\int d^4q\frac{1}{(2\pi)^4}G(\mathbf{p}',q)\frac{i}{\not q+\mu_1\not P-m+i\epsilon}\frac{i}{-q_0+\mu_2E-M-\mathbf{q}^2/2M+i\epsilon}$$
$$\times G(q,\mathbf{p})\frac{1}{\not p_1-m+i\epsilon}+\cdots . \tag{2.5}$$

We may also define $V_{\text{eff}}$ through the equation

$$\tilde{K}_{Pb}(\mathbf{p}',\mathbf{p})=\frac{1}{\not p_3-m+i\epsilon}V_{\text{eff}}(\mathbf{p}',\mathbf{p})\frac{1}{\not p_1-m+i\epsilon}$$
$$+\frac{1}{\not p_3-m+i\epsilon}\int d^3q\frac{1}{(2\pi)^3}V_{\text{eff}}(\mathbf{p}',\mathbf{q})\frac{i}{\not q+\mu_1\not P-m+i\epsilon}V_{\text{eff}}(\mathbf{q},\mathbf{p})\frac{1}{\not p_1-m+i\epsilon}+\cdots , \tag{2.6}$$

where $p_{30}$, $p_{10}$, and $q_0$ are all fixed by the mass-shell constraints. Next we expand both $G$ and $V_{\text{eff}}$ in powers of coupling strength. Thus

$$G=G^{(2)}+G^{(4)}+G^{(6)}+\cdots ,$$
$$V_{\text{eff}}=V_{\text{eff}}^{(2)}+V_{\text{eff}}^{(4)}+V_{\text{eff}}^{(6)}+\cdots . \tag{2.7}$$

The calculation of $V_{\text{eff}}$ proceeds order by order in perturbation theory and is carried out by requiring the scattering amplitudes to be identical whether calculated using $G$ or $V_{\text{eff}}$. Thus, leaving out external electron factors, the scattering amplitude consists of

$$G^{(2)}(\mathbf{p}',\mathbf{p})+G^{(4)}(\mathbf{p}',\mathbf{p})+G^{(6)}(\mathbf{p}',\mathbf{p})+\cdots$$
$$+\int d^4q\frac{1}{(2\pi)^4}[G^{(2)}(\mathbf{p}',q)+\cdots]\frac{i}{\not q+\mu_1\not P-m+i\epsilon}\frac{i}{-q_0+\mu_2E-M-\mathbf{q}^2/2M+i\epsilon}$$
$$\times[G^{(2)}(q,\mathbf{p})+G^{(4)}(q,\mathbf{p})+\cdots]+\cdots\ , \tag{2.8}$$

where the first line sums all irreducible diagrams. This is followed by irreducible diagrams occurring twice with two-particle propagation between interactions. The series continues, generating all Feynman diagrams for a Dirac electron interacting with a nonrelativistic spinless nucleus.

The scattering amplitude calculated through use of $V_{\rm eff}$ consists of the complete Born series, written as

$$V_{\rm eff}^{(2)}(\mathbf{p}',\mathbf{p})+V_{\rm eff}^{(4)}(\mathbf{p}',\mathbf{p})+V_{\rm eff}^{(6)}(\mathbf{p}',\mathbf{p})+\cdots$$
$$+\int d^3q\frac{1}{(2\pi)^3}[V_{\rm eff}^{(2)}(\mathbf{p}',\mathbf{q})+V_{\rm eff}^{(4)}(\mathbf{p}',\mathbf{q})+\cdots]\frac{i}{\not q+\mu_1\not P-m+i\epsilon}[V_{\rm eff}^{(2)}(\mathbf{q},\mathbf{p})+V_{\rm eff}^{(4)}(\mathbf{q},\mathbf{p})+\cdots]+\cdots\ , \tag{2.9}$$

where $q_0=m+\epsilon-\mathbf{q}^2/2M$.

The construction of $V_{\rm eff}$ is illustrated as follows:

$$V_{\rm eff}^{(2)}=G^{(2)}\ ,$$
$$V_{\rm eff}^{(4)}=G^{(4)}+(G^{(2)}iSiDG^{(2)}-V_{\rm eff}^{(2)}iSV_{\rm eff}^{(2)})\ , \tag{2.10}$$

where $S$ is the electron propagator and $D$ is the nuclear propagator. We have enclosed a portion of $V_{\rm eff}^{(4)}$ in parentheses and will show later how the indicated subtraction can most readily be implemented. Note that when Eq. (2.10) is used in Eq. (2.9), retaining *only* terms to fourth order in the coupling, the result coincides with the fourth-order terms of the exact amplitude of Eq. (2.8). To proceed to the next correction we construct

$$V_{\rm eff}^{(6)}=G^{(6)}+G^{(4)}iSiDG^{(2)}+G^{(2)}iSiDG^{(4)}$$
$$+G^{(2)}iSiDG^{(2)}iSiDG^{(2)}-V_{\rm eff}^{(4)}iSV_{\rm eff}^{(2)}$$
$$-V_{\rm eff}^{(2)}iSV_{\rm eff}^{(4)}-V_{\rm eff}^{(2)}iSV_{\rm eff}^{(2)}iSV_{\rm eff}^{(2)}\ . \tag{2.11}$$

It is straightforward to see that with this correction the potential scattering result of Eq. (2.9), calculated to third Born approximation, will give the correct amplitude of Eq. (2.8) through sixth order. The process of constructing additional corrections $V_{\rm eff}^{(2n)}$ $(n>3)$ can be continued order by order, but clearly the complexity increases as $n$ increases.

To proceed further in Eq. (2.10), (2.11), or in any further terms which may be required, we proceed by schematically writing

$$D=\delta+\Delta\ . \tag{2.12}$$

For example,

$$D(q)=\frac{1}{-q_0+\mu_2E-M-\frac{\mathbf{q}^2}{2M}+i\epsilon}$$
$$=\left[-2\pi i\delta\left[-q_0+\mu_2E-M-\frac{\mathbf{q}^2}{2M}\right]\right.$$
$$\left.+\left[-q_0+\mu_2E-M-\frac{\mathbf{q}^2}{2M}-i\epsilon\right]^{-1}\right]\ . \tag{2.13}$$

Thus $\delta$ is the Dirac delta-function part while $\Delta$ has the same form as $D$ except that the sign of $\epsilon$ is reversed. The advantage of the separation shown in Eqs. (2.12) and (2.13) is that the $\delta$ terms produce very important cancellations in the construction of $V_{\rm eff}$. For example, the $\delta$ term in Eq. (2.10) leads to a cancellation of $V_{\rm eff}^{(2)}iSV_{\rm eff}^{(2)}$ and consequently $G^{(2)}iSi\Delta G^{(2)}$ is the residual correction beyond the irreducible piece $G^{(4)}$. Similar cancellations occur in Eq. (2.11).

Our analysis will be carried out in the Coulomb gauge. Only terms of order $1/M$ will be retained in the contributions to $V_{\rm eff}$. Three types of interactions, Coulomb, convection, and "seagull," will be required. The appropriate vertices are shown in Fig. 1 on the nuclear side. On the electron side when there is a Coulomb interaction the vertex will be $-ie\gamma_0$, while when there is a convection (transverse) interaction we then have $-ie(\gamma_\perp)_i$. The propagation functions for electron and nucleus are those appropriate to Dirac and Schrödinger particles, for example, $S(p)=1/(\not p-m+i\epsilon)$ and $D(q)=1/(q_0+\mu_2\epsilon-\mathbf{q}^2/2M+i\epsilon)$. For the Coulomb interaction we use a propagator $1/\mathbf{k}^2$, while for the convection we use $-g_{ij}/(k^2+i\epsilon)$. In the process of constructing $V_{\rm eff}$ there will be propagation terms involving $D(q)$ which will be denoted in the usual way by a solid line (see Fig. 2). However, as previously mentioned, for purposes of carrying out subtractions we separate into a $\delta$ function and a residual piece $\Delta(q)$. We denote this latter term by a solid line with a dot on it.

With this notation we may now draw various contributions. We have $V_{\rm eff}/i$ given by the diagrams shown in

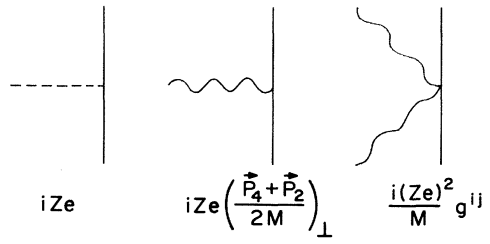


FIG. 1. Coulomb, convection, and seagull vertices.

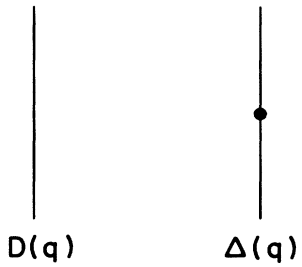


FIG. 2. Propagation function $D$ and residual part $\Delta$.

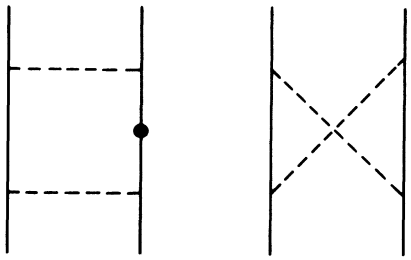

FIG. 4. Coulomb-Coulomb graphs.

Fig. 3. There is a major difficulty which arises from single-transverse interactions. It turns out that during the emission and subsequent absorption of a transverse photon an arbitrary number of Coulomb interactions can occur, all of which contribute to the same order in the energy. More specifically, corrections to the Breit potential can result in terms of order $(Z\alpha)^5 m^2/M$ to the energy and all of these involve arbitrary numbers of low momentum Coulomb interactions. A further discussion of this will be given later.

The major work in this type of approach entails the construction of the effective potential required for Eq. (2.4). Once it has been obtained the calculation of small energy shifts is carried out by means of conventional perturbation theory, using Dirac-Coulomb wave functions to describe the unperturbed state.

## III. LOWEST-ORDER RECOIL CORRECTIONS

The starting point of our approach, based on the formalism discussed in the preceding section, is the modified Dirac equation of Grotch and Yennie.[2] This equation, whose solution has been obtained, incorporates for $V_{\text{eff}}^{(2)}$ the Coulomb and convection interactions. The energy eigenvalues maintain the $2S_{1/2}$, $2P_{1/2}$ degeneracy except for small deviations proportional to $(m/M)^2(Z\alpha)^4$. The above degeneracy, which is predominantly broken by radiative corrections, is also broken by recoil effects beyond those already contained in the lower-order analysis. Thus it is necessary to correct the approximation which presumes that the effective potential consists only of the sum of Coulomb and convection potentials. Before proceeding to a more detailed analysis of recently calculated terms we review some earlier work which will set the stage for newer corrections.

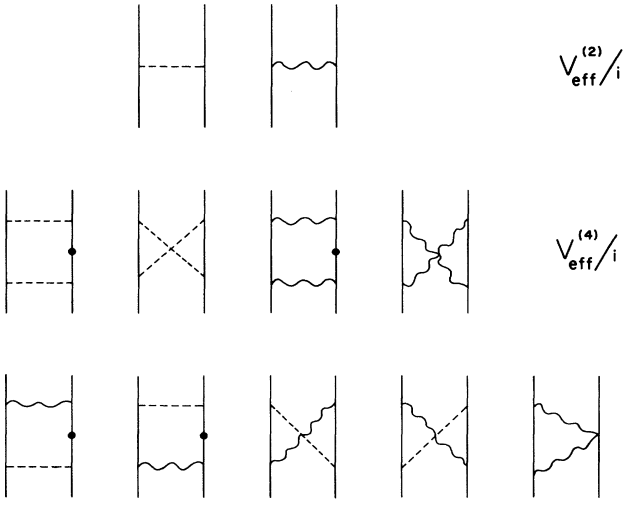


FIG. 3. Second-order and fourth-order contributions to $V_{\text{eff}}$.

### A. Coulomb-Coulomb corrections

The correction $V_{\text{eff}}^{(4)}$ must contain double-Coulomb exchange graphs. It is crucial to note, however, that the ladder Coulomb graphs contain terms which must be removed according to Eq. (2.10). The removal is readily accomplished by replacing $D$ of Eq. (2.13) by $\Delta$. This removes the positive-energy proton pole contribution, leaving a correction depicted in Fig. 4. In Ref. 2, this contribution led to a correction of order $(Z\alpha)^5 m^2/M$

$$\Delta E_{CC} = -\frac{4}{3}\frac{(Z\alpha)^2}{mM}|\psi_{2S}(0)|^2 \tag{3.1}$$

in agreement with earlier work.

### B. $\Delta E_T$ single-transverse photon correction

This correction has been a source of some difficulty because infinite-order perturbation theory (in the context of the approach of Sec. II) is necessary to obtain corrections of order $(Z\alpha)^5 m^2/M$. This occurs because during the transit time between emission and subsequent absorption of a transverse photon an arbitrary number of low-momentum Coulomb exchanges can occur, each contributing similarly to the energy shift. In view of this circumstance the correction is approached by an alternative method which we now describe.

In Ref. 2, in single-particle theory, the correction to the Breit potential is given as

$$-\frac{4\pi Z\alpha}{(2\pi)^3}\int d^3k\frac{1}{\mathbf{k}^2}\sum_m \frac{\langle n|\boldsymbol{\alpha}_e e^{i\mathbf{k}\cdot\mathbf{X}_e}|m\rangle\cdot\langle m|\boldsymbol{\alpha}_{p\perp}e^{-i\mathbf{k}\cdot\mathbf{X}_p}|n\rangle(E_n-E_m)}{E_n-E_m-k} . \tag{3.2a}$$

Although this expression will correctly yield recoil effects to order $(Z\alpha)^5m^2/M$ errors will result in higher orders due to the fact that negative-energy states are not correctly included in this formula. Corrections to Eq. (3.2a) above constitute a major objective of the present research.

After excluding negative-energy state contributions and proceeding to the nonrelativistic limit we obtain

$$\Delta E_T=\frac{-Z\alpha}{2\pi^2mM}\int d^3k\frac{1}{\mathbf{k}^2}\sum_m \frac{\langle n|\mathbf{p}_\perp e^{i\mathbf{k}\cdot\mathbf{r}}|m\rangle\langle m|[\mathbf{p},V]|n\rangle}{E_n-E_m-k} . \tag{3.2b}$$

To understand how Eq. (3.2b) has previously been calculated, we write

$$\begin{aligned}\frac{e^{i\mathbf{k}\cdot\mathbf{r}}}{E_n-E_m-k}&=\frac{1}{E_n-E_m-k}+\frac{e^{i\mathbf{k}\cdot\mathbf{r}}-1}{-k}\\&\quad+\frac{(e^{i\mathbf{k}\cdot\mathbf{r}}-1)(E_n-E_m)}{k(E_n-E_m-k)}\\&\equiv T_1+T_2+T_2' .\end{aligned} \tag{3.3}$$

The respective energy shifts are denoted by $\Delta E_{T_1}$, $\Delta E_{T_2}$, and $\Delta E_{T_2'}$. $\Delta E_{T_1}$ would be infrared divergent were it not for the energy difference appearing in the denominator. This term therefore produces a Bethe logarithm. $\Delta E_{T_1}$ and $\Delta E_{T_2}$ are separately ultraviolet divergent, but it is straightforward to see that their sum is finite. The results given previously are

$$\Delta E_{T_1}=\frac{8}{3}\frac{(Z\alpha)^2}{mM}|\psi_{2S}(0)|^2\ln\left|\frac{\Lambda}{(E_2-E_m)_{\rm av}}\right| , \tag{3.4}$$

$$\Delta E_{T_2}=\frac{8}{3}\frac{(Z\alpha)^2}{mM}|\psi_{2S}(0)|^2\left[\frac{25}{12}-\ln\frac{\Lambda}{mZ\alpha}\right] . \tag{3.5}$$

In Ref. 2, the sum of these terms was given as

$$\begin{aligned}&\Delta E_{T_1}+\Delta E_{T_2}\\&\quad=\frac{8}{3}\frac{(Z\alpha)^2}{mM}|\psi_{2S}(0)|^2\left[\frac{25}{12}+\ln\frac{mZ\alpha}{(E-E_m)_{\rm av}}\right] .\end{aligned} \tag{3.6}$$

This gave the pure recoil contribution from single-transverse photon to order $(Z\alpha)^5m^2/M$, and no corrections to this were given until rather recently when it became necessary to study higher-order terms.

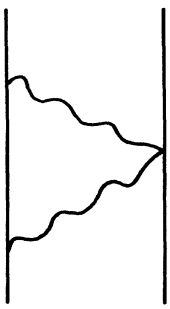

FIG. 5. Seagull correction.

### C. Two-transverse or seagull correction

The diagram which gives the leading correction is shown in Fig. 5.

The calculation of this contribution is somewhat subtle since one cannot ignore external momenta compared to the loop momentum without inducing an infrared divergence. Nevertheless, analysis of the above correction leads to the contribution

$$\Delta E_{TT}=\frac{2(Z\alpha)^2}{mM}|\psi_{2S}(0)|^2[\ln Z\alpha+\tfrac{7}{4}+\tfrac{4}{3}(1-\ln 2)] \tag{3.7}$$

of order $(Z\alpha)^5m^2/M$.

## IV. HIGHER-ORDER RECOIL OF ORDER $(Z\alpha)^6m^2/M$

We will now turn to a discussion of some previously published $(Z\alpha)^6m^2/M$ corrections before proceeding with newly calculated terms. Although much of what follows has already appeared in print the presentation given here is more pedagogic and complete.

### A. Double-Coulomb corrections

Equation (3.1) provided an energy shift from the double-Coulomb exchange graphs of Fig. 4. However, the result given relied on the approximation of setting the external momenta to zero compared to the internal loop momentum. According to Refs. 2–4, the double-Coulomb potential is

$$\begin{aligned}\delta V_{\rm dC}=-\int d^3p'\frac{1}{(2\pi)^3}\frac{m\gamma_0-E_{p'}+\boldsymbol{\alpha}\cdot\mathbf{p}'}{-2E_{p'}}\frac{-Ze^2}{(\mathbf{p}'-\mathbf{p}_3)^2}\\\times\frac{-Ze^2}{(\mathbf{p}_1-\mathbf{p}')^2}\frac{\mathbf{p}'^2+\mathbf{p}_1\cdot\mathbf{p}_3-\mathbf{p}'\cdot(\mathbf{p}_1+\mathbf{p}_3)}{M(m+E_{p'})^2} .\end{aligned} \tag{4.1}$$

We now evaluate this between free two-component spinors of momenta $\mathbf{p}_1$ and $\mathbf{p}_3$ to reduce to a form which can be evaluated using nonrelativistic wave functions. We then obtain

$$\Delta\tilde{V}_{\rm dC}=-\frac{1}{2M}\int d^3p'\frac{1}{(2\pi)^3}\frac{1}{E_{p'}(m+E_{p'})^3}\frac{-Ze^2}{(\mathbf{p}'-\mathbf{p}_3)^2}\frac{-Ze^2}{(\mathbf{p}_1-\mathbf{p}')^2}$$
$$\times\left[(\mathbf{p}'-\mathbf{p}_3)\cdot(\mathbf{p}'-\mathbf{p}_1)-\frac{E_{p'}-m}{2m}\mathbf{p}'\cdot(\mathbf{p}_1+\mathbf{p}_3)-\frac{1}{4m^2}[(m+E_{p'})^2-4m^2]\mathbf{p}_3\cdot\mathbf{p}_1\right]$$
$$\times[\mathbf{p}'^2-\mathbf{p}'\cdot(\mathbf{p}_1+\mathbf{p}_3)+\mathbf{p}_1\cdot\mathbf{p}_3]\ . \tag{4.2}$$

The terms of interest can have at most two powers of external momenta. In fact, the two powers must involve $\mathbf{p}_1$ or $\mathbf{p}_3$ quadratically. Thus the last term in both the large parentheses in the second line and the square brackets of the third can be dropped. We then write the product as

$$\mathbf{p}'^2(\mathbf{p}'-\mathbf{p}_3)\cdot(\mathbf{p}'-\mathbf{p}_1)+\mathbf{p}'^2\mathbf{p}'\cdot(\mathbf{p}_1+\mathbf{p}_3)\left[-1-\frac{E_{p'}-m}{2m}\right]+\mathbf{p}'\cdot(\mathbf{p}_1+\mathbf{p}_3)\mathbf{p}'\cdot(\mathbf{p}_1+\mathbf{p}_3)\left[1+\frac{E_{p'}-m}{2m}\right]$$
$$=\mathbf{p}'^2(\mathbf{p}'-\mathbf{p}_3)\cdot(\mathbf{p}'-\mathbf{p}_1)+\left[\frac{E_{p'}+m}{2m}\right][-\mathbf{p}'^2\mathbf{p}'\cdot(\mathbf{p}_1+\mathbf{p}_3)+\mathbf{p}'\cdot(\mathbf{p}_1+\mathbf{p}_3)\mathbf{p}'\cdot(\mathbf{p}_1+\mathbf{p}_3)]\ .$$

The term in square brackets contributes a higher order due to cancellations. The leading term can readily be evaluated since when the wave functions are introduced the integrals may easily be performed keeping $\mathbf{p}_1$ and $\mathbf{p}_3$ finite. When this is done, Eq. (3.1) is corrected to $\Delta E'_{CC}$ with

$$\Delta E'_{CC}=-\frac{4}{3}\frac{(Z\alpha)^2}{mM}|\psi_{2S}(0)|^2\left[1-\frac{3\pi Z\alpha}{8}\right]\ . \tag{4.3}$$

Thus to order $(Z\alpha)^6m^2/M$ we obtain an additional correction from the finiteness of the external momenta.

### B. Triple-Coulomb corrections

To carry out the calculation to this accuracy, we must also compute the effects of triple-Coulomb exchange.

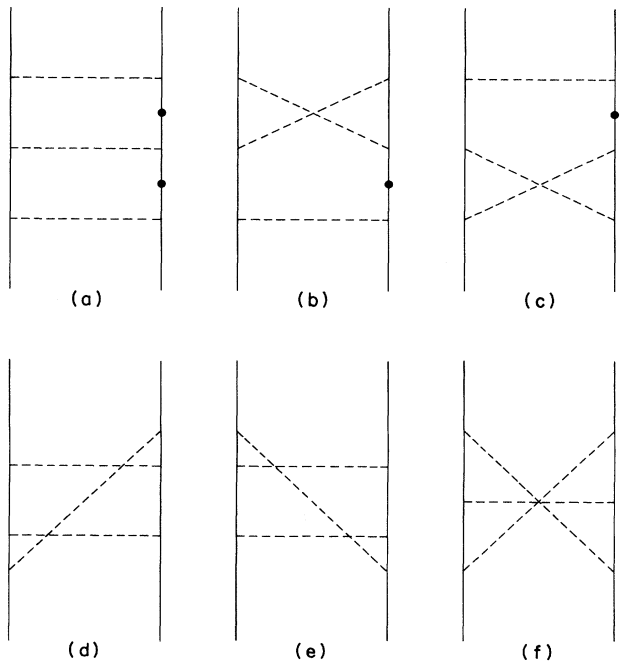


FIG. 6. Triple-Coulomb diagrams.

Upon examination of Eq. (2.11), substituting in Eq. (2.10) where necessary, we find the necessary Feynman diagrams and subtractions. These are shown in Fig. 6.

Choosing the Coulomb momenta, $q_1$, $q_2$, and $q_3$, as shown in Fig. 7, and setting all external three-momenta to zero (an approximation which will not affect the leading contribution), we write down the proton line structure, keeping in mind the proton pole subtraction. Equations (4.4a)–(4.4f) give the proton line structure for Figs. 6(a)–6(f), respectively,

$$i(Ze)^3\frac{1}{[-(q_3)_0-\mathbf{q}_3^2/2M-i\epsilon][(q_1)_0-\mathbf{q}_1^2/2M-i\epsilon]}\ , \tag{4.4a}$$

$$i(Ze)^3\frac{1}{[-(q_2)_0-\mathbf{q}_2^2/2M+i\epsilon][(q_1)_0-\mathbf{q}_1^2/2M-i\epsilon]}\ , \tag{4.4b}$$

$$i(Ze)^3\frac{1}{[-(q_3)_0-\mathbf{q}_3^2/2M-i\epsilon][(q_2)_0+\mathbf{q}_2^2/2M+i\epsilon]}\ , \tag{4.4c}$$

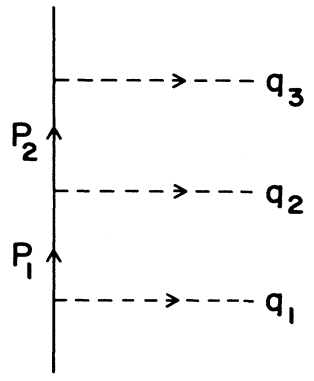


FIG. 7. Notation for Coulomb momenta.

$$i(Ze)^3\frac{1}{[-(q_1)_0-\mathbf{q}_1^2/2M+i\epsilon][(q_2)_0+\mathbf{q}_2^2/2M+i\epsilon]}\ , \tag{4.4d}$$

$$i(Ze)^3\frac{1}{[-(q_2)_0-\mathbf{q}_2^2/2M+i\epsilon][(q_3)_0-\mathbf{q}_3^2/2M+i\epsilon]}\ , \tag{4.4e}$$

$$i(Ze)^3\frac{1}{[-(q_1)_0-\mathbf{q}_1^2/2M+i\epsilon][(q_3)_0-\mathbf{q}_3^2/2M+i\epsilon]}\ . \tag{4.4f}$$

As the electron line structure, Coulomb propagators, and other factors, will be the same for each of these diagrams, we can combine proton line structures for Figs. 6(a) and 6(c) [Eq. (4.5a)], for Figs. 6(b) and 6(d) [Eq. (4.5b)], and for Figs. 6(e) and 6(f) [Eq. (4.5c)]:

$$i(Ze)^3\left[\frac{1}{[(q_1)_0-\mathbf{q}_1^2/2M-i\epsilon][(q_2)_0-\mathbf{q}_1^2/2M-i\epsilon]}-\frac{\mathbf{q}_1\cdot\mathbf{q}_2}{M}\frac{1}{[(q_3)_0+i\epsilon][(q_1)_0-i\epsilon][(q_2)_0-i\epsilon]}\right.$$
$$\left.-\frac{(-2\pi i)\delta((q_2)_0-\mathbf{q}_2^2/2M)}{[(q_3)_0+\mathbf{q}_3^2/2M+i\epsilon]}\right]\ , \tag{4.5a}$$

$$i(Ze)^3\left[-\frac{1}{[(q_1)_0-\mathbf{q}_1^2/2M-i\epsilon][(q_2)_0-\mathbf{q}_2^2/2M-i\epsilon]}-\frac{1}{[(q_1)_0+\mathbf{q}_1^2/2M-i\epsilon][(q_2)_0-\mathbf{q}_2^2/2M-i\epsilon]}\right.$$
$$\left.-\frac{(-2\pi i)\delta((q_2)_0-\mathbf{q}_2^2/2M))}{[(q_1)_0+\mathbf{q}_1^2/2M-i\epsilon]}\right]\ , \tag{4.5b}$$

$$i(Ze)^3\left[\frac{1}{[(q_1)_0+\mathbf{q}_1^2/2M-i\epsilon][(q_2)_0+\mathbf{q}_2^2/2M-i\epsilon]}-\frac{\mathbf{q}_1\cdot\mathbf{q}_2}{M}\frac{1}{[(q_3)_0+i\epsilon][(q_1)_0-i\epsilon][(q_2)_0-i\epsilon]}\right]\ . \tag{4.5c}$$

Finally, the proton line structure is given by

$$i(Ze)^3\frac{(-2\pi i)\delta((q_2)_0)}{[(q_1)_0-i\epsilon]^2}\frac{\mathbf{q}_1\cdot(\mathbf{q}_1+\mathbf{q}_2)}{M}=i(Ze)^3\frac{\mathbf{p}_1'\cdot\mathbf{p}_2'}{M}\frac{(-2\pi i)\delta((p_1')_0-(p_2')_0)}{[(p_1')_0-m+i\epsilon]^2}\ . \tag{4.6}$$

In deriving Eq. (4.5) from (4.1), only terms of lowest order in $1/M$ have been kept; in deriving Eq. (4.6) from Eq. (4.5), only terms of lowest order in $1/M$ have been kept, and energy momentum conservation $q_1^\mu+q_2^\mu+q_3^\mu=0$ ($\mu=0,1,2,3$) was used. $p_1'^\mu$ in Eq. (4.6) refer to the internal electron line momenta, as shown in Fig. 7.

Now, we can combine the proton line structure with the electron line structure and propagators, to give $V_{\rm eff}^{(6)}$:

$$V_{\rm eff}^{(6)}(CCC)=i\int d^4p_1'd^4p_2'\frac{1}{(2\pi)^8}\left[\frac{i}{\mathbf{p}_1'^2}\frac{i}{(\mathbf{p}_1'-\mathbf{p}_2')^2}\frac{i}{\mathbf{p}_2'^2}\right]\left[i(Ze)^3\frac{\mathbf{p}_1'\cdot\mathbf{p}_2'}{M}\frac{(-2\pi i)\delta((p_1')_0-(p_2')_0)}{[(p_1')_0-m+i\epsilon]^2}\right]$$
$$\times\left[\bar u(0)\frac{(-ie\gamma_0)i}{\not p_1'-m+i\epsilon}(-ie\gamma_0)\frac{i}{\not p_2'-m+i\epsilon}(-ie\gamma_0)u(0)\right]$$
$$=i\int d^4p_1'd^4p_2'\frac{1}{(2\pi)^8}\left[\frac{i}{\mathbf{p}_1'^2}\frac{i}{(\mathbf{p}_1'-\mathbf{p}_2')^2}\frac{i}{\mathbf{p}_2'^2}\right]\left[i(Ze)^3\frac{\mathbf{p}_1'\cdot\mathbf{p}_2'}{M}\frac{(-2\pi i)\delta((p_1')_0-(p_2')_0)}{[(p_1')_0-m+i\epsilon]^2}\right]$$
$$\times\left[-ie^3\frac{[(p_2')_0+m][(p_1')_0+m]+\mathbf{p}_1'\cdot\mathbf{p}_2'}{[(p_2')_0-E_2'+i\epsilon][(p_2')_0+E_2'-i\epsilon][(p_1')_0-E_1'+i\epsilon][(p_1')_0+E_1'-i\epsilon]}\right]$$
$$=\frac{(Z\alpha)^3}{2\pi^3M}\int d^3p_1'd^3p_2'\frac{1}{\mathbf{p}_1'^2(\mathbf{p}_1'-\mathbf{p}_2')^2\mathbf{p}_2'^2}\frac{\mathbf{p}_1'\cdot\mathbf{p}_2'}{\mathbf{p}_1'^2-\mathbf{p}_2'^2}\left[\frac{(m-E_2')^2+\mathbf{p}_1'\cdot\mathbf{p}_2'}{E_2'(m+E_2')^2}-\frac{(m-E_1')^2+\mathbf{p}_1'\cdot\mathbf{p}_2'}{E_1'(m+E_1')^2}\right]\ , \tag{4.7}$$

where $E_1'=(\mathbf{p}_1'^2+m^2)^{1/2}$ and $E_2=(\mathbf{p}_2'^2+m^2)^{1/2}$.

Equation (4.7) can be integrated analytically, to some approximation, with the result

$$V_{\rm eff}^{(6)}(CCC)=\frac{(Z\alpha)^3}{mM}\frac{\pi}{2}\ . \tag{4.8a}$$

As a test, we can also integrate Eq. (4.7) "exactly" using the Monte Carlo integration program VEGAS, with the result

$$V_{\rm eff}^{(6)}(CCC)=\frac{(Z\alpha)^3}{mM}\frac{4}{\pi}(1.232\pm0.002)\ , \tag{4.8b}$$

where $\cos\theta=\mathbf{p}_1'\cdot\mathbf{p}_2'/p_1'p_2'$, and the $\phi_1$ and $\Omega_2$ integrals were performed analytically. The two results agree to

within the error. Therefore

$$\Delta E(CCC)=|\psi_{2S}(0)|^2 V_{\rm eff}^{(6)}(CCC)$$
$$=-\frac{4}{3}\frac{(Z\alpha)^2}{mM}|\psi_{2S}(0)|^2\left[-\frac{3\pi Z\alpha}{8}\right]. \quad (4.9)$$

Combining this with Eqs. (3.1) and (4.3), we obtain the recoil contribution of pure Coulomb graphs as

$$\Delta E_{\rm Coul\ rec}=-\frac{4}{3}\frac{(Z\alpha)^2}{mM}|\psi_{2S}(0)|^2\left[1-\frac{3\pi Z\alpha}{4}\right]. \quad (4.10)$$

### C. Seagull and Coulomb

The necessary Feynman diagrams for this contribution are also present in Eq. (2.11). The $G^{(6)}$ contributions are shown in Figs. 8(b), 8(c), 8(e), and 8(f) [irreducible diagrams contributing to $O((Z\alpha)^6)$]; the $(G^{(4)}iSiDG^{(2)}-V_{\rm eff}^{(4)}iSV_{\rm eff}^{(2)}$ and $(G^{(2)}iSiDG^{(4)}-V_{\rm eff}^{(2)}iSV_{\rm eff}^{(4)}$ contributions are shown in Figs. 8(d) and 8(a), respectively; there is no $(G^{(2)}iSiDG^{(2)}iSiDG^{(2)}-V_{\rm eff}^{(2)}iSV_{\rm eff}^{(2)}iSV_{\rm eff}^{(2)})$ contribution, as the seagull diagram itself has four powers of coupling.

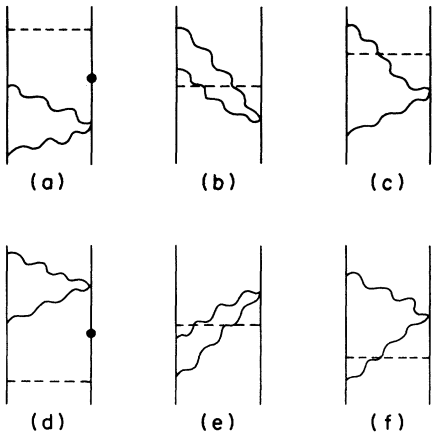


FIG. 8. Diagrams with single Coulomb and a seagull.

All of the Feynman diagrams will be of the form

$$\int d^4q_1 d^4q_2 d^4q_3 \frac{1}{(2\pi)^{12}}(2\pi)^4\delta^4(q_1+q_2+q_3)[\bar{u}(-ie\gamma_0)(iS)(-ie\gamma_{\perp q_1})_l(iS)(-ie\gamma_{\perp q_2})_m u]$$
$$\times\{+iZeD[+i(Ze)^2 g_{ij}]\}\left[\frac{-ig_{li}}{q_1^2+i\epsilon}\frac{-ig_{mj}}{q_2^2+i\epsilon}\frac{+i}{\mathbf{q}_3^2}\right]. \quad (4.11a)$$

We can move all metric factors onto the electron line structure

$$\int d^4q_1 d^4q_2 d^4q_3 \frac{1}{(2\pi)^{12}}(2\pi)^4\delta^4(q_1+q_2+q_3)[\bar{u}(-ie\gamma_0)(iS)(-ie\boldsymbol{\gamma}_{\perp q_1})\cdot(iS)(-ie\boldsymbol{\gamma}_{\perp q_2})u]$$
$$\times\{(+iZe)(iD)[+i(Ze)^2]\}\left[\frac{-i}{q_1^2+i\epsilon}\frac{-i}{q_2^2+i\epsilon}\frac{+i}{\mathbf{q}_3^2}\right]. \quad (4.11b)$$

There are two different proton line structures, $P_{1,\pm\epsilon}$ [Figs. 8(a)–8(c)] and $P_{2,\pm\epsilon}$ [Figs. 8(d)–8(f)], where $\pm\epsilon$ refers to the sign of $i\epsilon$ in the proton propagator. There are three different electron line structures $L_1$ [Figs. 8(a) and 8(e)], $L_2$ [Figs. 8(c) and 8(f)], and $L_3$ [Figs. 8(b) and 8(d)]. The total contribution is

$$L_1(P_{1,-\epsilon}+P_{2,+\epsilon})+L_2(P_{1,+\epsilon}+P_{2,+\epsilon})+L_3(P_{1,+\epsilon}+P_{2,-\epsilon}).$$

It is easy to see that

$$P_{1,+\epsilon}=i\frac{(Ze)^3}{M}\frac{1}{(q_3)_0-i\epsilon}, \quad (4.12a)$$

$$P_{2,+\epsilon}=-i\frac{(Ze)^3}{M}\frac{1}{(q_3)_0+i\epsilon}, \quad (4.12b)$$

to lowest order in $1/M$. It is apparent that $(P_{1,\pm\epsilon}+P_{2,\mp\epsilon})=0$, and so only the $L_2$ term contributes. $(P_{1,+\epsilon}+P_{2,+\epsilon})=-i(Ze)^3(-2\pi i)\delta((q_3)_0)/M$.

The necessary electron line structure is

$$L_2=-\bar{u}(0)(-ie\gamma_{\perp q_1})\frac{i}{\not p_2'-m+i\epsilon}(-ie\gamma_0)\frac{i}{\not p_1'-m+i\epsilon}\cdot(-ie\gamma_{\perp q_2})u(\mathbf{p})$$

$$=ie^3\left[\frac{[m-(p_1')_0][m-(p_2')_0][1+(\mathbf{p}_1'\cdot\mathbf{p}_2')^2/p_1'^2p_2'^2]+2\mathbf{p}_1'\cdot\mathbf{p}_2'}{[(p_1')_0-E_1'+i\epsilon][(p_1')_0+E_1'-i\epsilon][(p_2')_0-E_2'+i\epsilon][(p_2')_0+E_2'-i\epsilon]}\right]. \tag{4.13}$$

Therefore, in terms of the internal electron line momenta, the contribution to $V_{\rm eff}^{(6)}$ from seagull-Coulomb (SC) is

$$V_{\rm eff}^{(6)}({\rm SC})=\frac{-i(Z\alpha)^3}{2\pi^4M}\int d^4p_1'd^4p_2'\frac{\delta((p_1')_0-(p_2')_0)}{\{[(p_1')_0-m]^2-\mathbf{p}_1'^2+i\epsilon\}\{[(p_2')_0-m]^2-\mathbf{p}_2'^2+i\epsilon\}(\mathbf{p}_1'-\mathbf{p}_2')^2}$$

$$\times\left[\frac{[m-(p_1')_0][m-(p_2')_0][1+(\mathbf{p}_1'\cdot\mathbf{p}_2')^2/\mathbf{p}_1'^2\mathbf{p}_2'^2]+2\mathbf{p}_1'\cdot\mathbf{p}_2'}{[(p_1')_0-E_1'+i\epsilon][(p_1')_0+E_1'-i\epsilon][(p_2')_0-E_2'+i\epsilon][(p_2')_0+E_2'-i\epsilon]}\right]. \tag{4.14}$$

Here the $(p_1')_0$ and $(p_2')_0$ integrals can be performed analytically, along with the $\Omega_2$ and $\phi_1$ integrals. Again, we choose $\cos\theta_1=\mathbf{p}_1'\cdot\mathbf{p}_2'/p_1'p_2'$, and the remaining three-dimensional integral can be performed using VEGAS, with the results

$$V_{\rm eff}^{(6)}({\rm SC})=\frac{(Z\alpha)^3}{mM}\frac{2}{\pi}(3.799\pm0.004) \tag{4.15}$$

and

$$\Delta E({\rm SC})=\frac{(Z\alpha)^6m^2}{M}\frac{2}{n^3\pi^2}(3.799\pm0.004)\,. \tag{4.16}$$

This result has been previously published.[5]

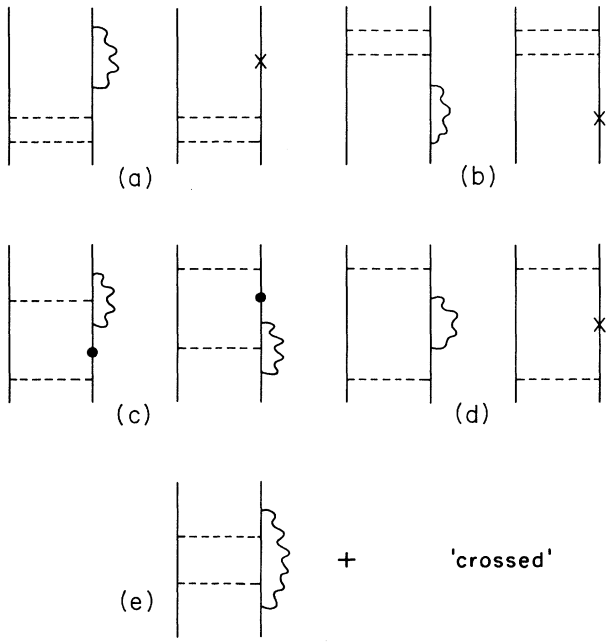


FIG. 9. Radiative corrections on the proton line with double-Coulomb exchange.

### D. Finite proton size

The contributions we estimate have been previously discussed. For completeness we include a short discussion here. We begin with Fig. 9. These are the two Coulomb exchange diagrams, with a radiated photon or pion inserted on the proton line everywhere possible. First, as we consider the external proton to be approximately on shell, Figs. 9(a) and 9(b) do not contribute, as an external self-energy plus counter-term is identically zero. Second, we can treat the radiated photon in the Coulomb gauge (although the results are gauge independent). In that case, the radiated Coulomb photon does not contribute, as we can always choose the contour for the $k_0$ integration so that no poles are enclosed ($k$ refers to the momentum of the radiated particle). Thus we need only consider a radiated transverse photon.

We naively expect that the remaining diagrams, with a radiated transverse photon, will be of order $Z^2\alpha(Z\alpha)^5m^3/M^2$, but there is a possibility that factors of proton mass will appear in the numerator, in the course of performing the loop integrals. A thorough analysis demonstrates that our naive expectation is correct, and, therefore, that the contribution of these diagrams is negligible. A more careful analysis,[5] treating the proton relativistically yields the same result, as well as the result for the corresponding diagrams with a radiated pion contributing, at most, to order $Z^2\alpha_s(Z\alpha)^5m^2/M$.

### E. Single-transverse $\Delta E_{T_2'}'$

This correction comes from the third term of Eq. (3.3) and represents a $(Z\alpha)^6m^2/M$ contribution which can be evaluated analytically. It should be kept in mind that Eq. (3.2a) is an approximation and it is important, as stressed by Sapirstein and Yennie, to go beyond that approximation. This will be done in Sec. V in which an extensive analysis of the single-transverse recoil, including new corrections, will be carried out. Returning to $\Delta E_{T_2'}'$ we find

$$\Delta E_{T_2'}=\frac{Z\alpha}{2\pi^2 mM}\int d^3k\frac{1}{k^3}\sum_m \frac{\langle n|\mathbf{p}_\perp(e^{i\mathbf{k}\cdot\mathbf{r}}-1)|m\rangle\cdot\langle m|\mathbf{p}|n\rangle(E_n-E_m)^2}{E_n-E_m-k} . \tag{4.17}$$

To evaluate this we use

$$\begin{aligned}\langle m|\mathbf{p}|n\rangle(E_n-E_m)^2&=\left\langle m\left|\left[\left[\mathbf{p},\frac{\mathbf{p}^2}{2m}+V\right],\frac{\mathbf{p}^2}{2m}+V\right]\right|n\right\rangle\\&=\left\langle m\left|\left[[\mathbf{p},V],\frac{\mathbf{p}^2}{2m}\right]\right|n\right\rangle\end{aligned} \tag{4.18}$$

and

$$\begin{aligned}\frac{1}{E_n-E_m-k}|m\rangle&=\frac{1}{E_n-(\mathbf{p}^2/2m+V)-k}|m\rangle\\&=\frac{-2m}{\mathbf{p}^2+2mk+2mV+\gamma^2}|m\rangle .\end{aligned} \tag{4.19}$$

Thus, removing the sum on states, we find

$$\Delta E_{T_2'}=\frac{Z\alpha}{2\pi^2 mM}\int d^3k\frac{1}{k^3}\left\langle n\left|\mathbf{p}_\perp(e^{i\mathbf{k}\cdot\mathbf{r}}-1)\frac{1}{\mathbf{p}^2+2mk+2mV+\gamma^2}\cdot[\mathbf{p}^2,[\mathbf{p},V]]\right|n\right\rangle . \tag{4.20}$$

We expect contributions to come from high momenta and consequently to the desired accuracy the denominator can be simplified by dropping $2mV+\gamma^2$. We may then evaluate (4.20) in the momentum representation. It is straightforward to simplify to

$$\begin{aligned}\Delta E_{T_2'}=&\frac{-16(Z\alpha)^3|\psi_{2S}(0)|^2}{M}\\&\times\int d^3k\frac{1}{k^3}d^3p\frac{1}{(2\pi)^3}\frac{\mathbf{p}_\perp\cdot\mathbf{p}}{\mathbf{p}^4}\\&\times\left[\frac{1}{(\mathbf{p}-\mathbf{k})^2+2mk}-\frac{1}{\mathbf{p}^2+2mk}\right] .\end{aligned} \tag{4.21}$$

The integral is readily carried out by first integrating over $p$, then integrating with respect to $k$ and finally with respect to the angle between $\mathbf{p}$ and $\mathbf{k}$. The final result is

$$\Delta E_{T_2'}=-\frac{4}{3}\frac{(Z\alpha)^2}{mM}|\psi_{2S}(0)|^2\left[-\frac{9\pi}{4}Z\alpha\right] . \tag{4.22}$$

We now combine this with Eq. (3.7) to obtain

$$\begin{aligned}\Delta E_{T_1}+\Delta E_{T_2}+\Delta E_{T_2}'=&\frac{8}{3}\frac{(Z\alpha)^2}{mM}|\psi_{2S}(0)|^2\\&\times\left[\ln\left[\frac{mZ\alpha}{\Delta E}\right]+\frac{25}{12}+\frac{9}{8}\pi Z\alpha\right] ,\end{aligned} \tag{4.23}$$

where $\Delta E$ is the average excitation energy. This result is given in Ref. 4. The corresponding result for $P$ states is negligible.

### F. Seagull correction

To evaluate the seagull term shown in Fig. 5, we make approximations. Let us return to the original expression which led to Eq. (3.7) and analyze this in detail.

We begin with the expression

$$\Delta V_{TT}=\frac{(Z\alpha)^2}{mM}\int d^4p\frac{1}{\pi^2 i}\frac{(-m)(p_0-m)\boldsymbol{\delta}_{\perp 1}\cdot\boldsymbol{\delta}_{\perp 3}}{[(p-p_3)^2+i\epsilon][(p-p_1)^2+i\epsilon](p^2-m^2+i\epsilon)} , \tag{4.24}$$

where

$$\boldsymbol{\delta}_{\perp 1}\cdot\boldsymbol{\delta}_{\perp 3}=1+\cos^2\theta_{q_1q_2}=2-\sin^2\theta_{q_1q_2}=2-\frac{(\mathbf{q}_1\times\mathbf{q}_3)^2}{\mathbf{q}_1^2\mathbf{q}_3^2} .$$

Let $p_0-m\equiv i\eta$ and use

$$\int d^4p\frac{1}{\pi^2 i}=\frac{1}{\pi^2}\int d^3p\int_{-\infty}^{\infty}d\eta .$$

With these changes

$$\frac{1}{(p-p_3)^2}\frac{1}{(p-p_1)^2}=\frac{1}{\eta^2+\mathbf{q}_3^2}\frac{1}{\eta^2+\mathbf{q}_1^2}\ ,$$

$$\frac{-m(p_0-m)}{p^2-m^2}=\frac{i\eta m}{-2mi\eta+\eta^2+\mathbf{p}^2}=\frac{1}{2}\left[-1+\frac{\eta^2+\mathbf{p}^2}{-2mi\eta+\eta^2+\mathbf{p}^2}\right].$$

Equation (4.24) now becomes

$$\Delta V_{TT}=\frac{(Z\alpha)^2}{mM}\frac{1}{\pi^2}\int d^3p\int_{-\infty}^{\infty}d\eta\left[2-\frac{(\mathbf{q}_1\times\mathbf{q}_3)^2}{\mathbf{q}_1^2\mathbf{q}_3^2}\right]\frac{1}{\eta^2+\mathbf{q}_1^2}\frac{1}{\eta^2+\mathbf{q}_1^2}\frac{1}{2}\left[-1+\frac{(\eta^2+\mathbf{p}^2)^2}{4m^2\eta^2+(\eta^2+\mathbf{p}^2)^2}\right] \tag{4.25}$$

or

$$\Delta V_{TT}=-\frac{(Z\alpha)^2}{mM\pi^2}\int d^3p\int_{-\infty}^{\infty}d\eta\left[1-\frac{(\mathbf{q}_1\times\mathbf{q}_2)^2}{2\mathbf{q}_1^2\mathbf{q}_3^2}\right]\left[\left[\frac{1}{\eta^2+\mathbf{q}_3^2}\frac{1}{\eta^2+\mathbf{q}_1^2}-\frac{1}{4m^2\eta^2+(\eta^2+\mathbf{p}^2)^2}\right]\right.$$
$$\left.-\frac{(\eta^2+\mathbf{p}^2)^2}{4m^2\eta^2+(\eta^2+\mathbf{p}^2)^2}\left[\frac{1}{(\eta^2+\mathbf{q}_3^2)(\eta^2+\mathbf{q}_1^2)}-\frac{1}{(\eta^2+\mathbf{p}^2)^2}\right]\right]. \tag{4.26}$$

We now separate this into low-order and high-order contributions by writing

$$\Delta V_{TT}=\Delta V_{TT}^{L1}+\Delta V_{TT}^{L2}+\Delta V_{TT}^{H}\ , \tag{4.27}$$

with

$$\Delta V_{TT}^{L1}=\frac{-(Z\alpha)^2}{mM\pi^2}\int d^3p\int_{-1}^{1}d\eta\left[\frac{1}{(\eta^2+\mathbf{q}_3^2)(\eta^2+\mathbf{q}_1^2)}-\frac{1}{4m^2\eta^2+(\eta^2+\mathbf{p}^2)^2}\right], \tag{4.28a}$$

$$\Delta V_{TT}^{L2}=\frac{(Z\alpha)^2}{mM\pi^2}\int d^3p\int_{-1}^{1}d\eta\frac{1}{(\eta^2+\mathbf{q}_3^2)(\eta^2+\mathbf{q}_1^2)}\frac{(\mathbf{q}_1\times\mathbf{q}_3)^2}{2\mathbf{q}_1^2\mathbf{q}_3^2}\ , \tag{4.28b}$$

$$\Delta V_{TT}^{H}=\frac{(Z\alpha)^2}{mM\pi^2}\int d^3p\int_{-1}^{1}d\eta\frac{1}{4m^2\eta^2+(\eta^2+\mathbf{p}^2)^2}\left[\left[\frac{(\eta^2+\mathbf{p}^2)^2}{(\eta^2+\mathbf{q}_1^2)(\eta^2+\mathbf{q}_3^2)}-1\right]-\frac{(\eta^2+\mathbf{p}^2)^2}{(\eta^2+\mathbf{q}_1^2)(\eta^2+\mathbf{q}_3^2)}\frac{(\mathbf{q}_1\times\mathbf{q}_3)^2}{2\mathbf{q}_1^2\mathbf{q}_3^2}\right]. \tag{4.28c}$$

The integrals above can be carried out to sufficient accuracy. We shall not discuss the details. For $S$ states we obtain

$$\Delta E_{TT}^{L1}=\frac{2(Z\alpha)^2}{mM}|\psi(0)|^2\times\left[\ln Z\alpha+\left[\ln\frac{2}{n}+\sum_{1}^{n}\frac{1}{i}+\frac{n-1}{2n}\right]\right], \tag{4.29a}$$

$$\Delta E_{TT}^{L2}=\frac{2(Z\alpha)^2}{mM}|\psi(0)|^2[\tfrac{4}{3}(1-\ln 2)]\ , \tag{4.29b}$$

$$\Delta E_{TT}^{H}=\frac{2(Z\alpha)^2}{mM}|\psi(0)|^2\left[-\frac{\pi}{2}Z\alpha\ln\frac{2}{Z\alpha}-\frac{3\pi Z\alpha}{4}\right]. \tag{4.29c}$$

Equation (4.29a) is the generalization to arbitrary $n$ of (4.36) of Ref. 2. For $n=2$ Eqs. (4.29a) and (4.29b) account for Eq. (3.7) while Eq. (4.29c) provides a more recently calculated higher-order correction. For $n=2$ the sum of results for the transverse-transverse ($TT$) or seagull terms is

$$\Delta E'_{TT}=\frac{4(Z\alpha)^2}{3mM}|\psi(0)|^2\left[\tfrac{3}{2}(\ln Z\alpha+\tfrac{7}{4})+2(1-\ln 2)-\frac{3\pi}{4}Z\alpha\ln\frac{2}{Z\alpha}-\frac{9\pi Z\alpha}{8}\right]. \tag{4.30}$$

## V. NEW SINGLE-TRANSVERSE CORRECTIONS

In this section we will first review in greater detail the original single-transverse photon correction to the Lamb shift and then discuss two new and significant corrections. The new corrections are contained in the single-Coulomb–single-transverse graphs (we keep external momenta nonzero everywhere) and the double-Coulomb–single-transverse graphs (here we set external momenta to zero). The necessity for the first of these corrections was pointed out to us by Sapirstein and Yennie.[6]

Before discussing these new contributions we must relate the language and notation of old-fashioned perturbation theory of the original single-transverse calculation to the Feynman diagram approach discussed earlier in this

paper. The calculation of diagrams containing only a single-transverse photon is more difficult than the calculation of diagrams that involve only Coulomb exchange or those that involve seagull plus Coulomb. There are many subtleties due to the fact that the calculation of the single-transverse exchange in old-fashioned perturbation theory contains diagrams with an infinite number of Coulomb interactions. Thus it already sums an infinite subset of Feynman diagrams.

### A. Original single-transverse calculation

In old-fashioned perturbation theory the energy shift due to emission and absorption of a transverse photon is

$$\Delta E_0=-\frac{2Ze^2}{(2\pi)^3}\int d^3k\frac{1}{2k}\sum_m\frac{\langle n|\boldsymbol{\alpha}_{e\perp}e^{i\mathbf{k}\cdot\mathbf{X}_e}|m\rangle\langle m|\boldsymbol{\alpha}_p e^{-i\mathbf{k}\cdot\mathbf{X}_p}|n\rangle}{E_n-E_m-k}\ . \tag{5.1}$$

As mentioned earlier, this expression is not compatible with hole theory and will need to be corrected later. If the energy difference $E_n-E_m$ is ignored compared to $k$ the result is simply the Breit interaction. The correction to the Breit interaction is

$$\Delta E_T=\frac{-Z\alpha}{2\pi^2}\int d^3k\frac{1}{\mathbf{k}^2}\sum_m\frac{\langle n|\boldsymbol{\alpha}_{e\perp}e^{i\mathbf{k}\cdot\mathbf{X}_e}|m\rangle\langle m|\boldsymbol{\alpha}_p e^{-i\mathbf{k}\cdot\mathbf{X}_p}|n\rangle(E_n-E_m)}{E_n-E_m-k}\ . \tag{5.2}$$

In the literature the calculation of this expression has proceeded by replacing $\boldsymbol{\alpha}_e$ by $\mathbf{p}_e/m$ and $\boldsymbol{\alpha}_p$ by $\mathbf{p}_p/M$ and restricting the intermediate states to those of positive energy. This leads to

$$\Delta E_T=\frac{-Z\alpha}{2\pi^2 mM}\int d^3k\frac{1}{\mathbf{k}^2}\sum_m\frac{\langle n|\mathbf{p}_\perp e^{i\mathbf{k}\cdot\mathbf{r}}|m\rangle\langle m|[\mathbf{p},V]|n\rangle}{E_n-E_m-k}\ . \tag{5.3}$$

We have previously discussed the evaluation of Eq. (5.3) and shown how it leads to Eq. (4.23). However, Eq. (5.3) is an approximation which must be better understood if we are to examine additional corrections which might be present.

### B. Relation between old-fashioned perturbation theory and Feynman diagrammatic techniques

We begin with Eq. (5.3), which is independent of representation, and we now insert complete sets of momentum eigenstates to obtain

$$\Delta E_T=\frac{2(Z\alpha)^2}{\pi mM}\int d^3k\,d^3p_i d^3p_f d^3p'\frac{1}{\mathbf{k}^2(2\pi)^9}\phi_n^\dagger(\mathbf{p}_f)\times\frac{\mathbf{p}_{f\perp}\cdot(\mathbf{p}_i-\mathbf{p}')}{(\mathbf{p}_i-\mathbf{p}')^2}\times\left[\sum_m\frac{\phi_m(\mathbf{p}_f-\mathbf{k})\phi_m^\dagger(\mathbf{p}')}{E_n-E_m-k}\right]\phi_n(\mathbf{p}_i)\ . \tag{5.4}$$

The expression in large parentheses is

$$2m\tilde{G}_{\rm NR}(\mathbf{p}_f-\mathbf{k},\mathbf{p}';E_n-k)\ ,$$

where $\tilde{G}_{\rm NR}$ is the nonrelativistic momentum-space Coulomb Schrödinger propagator. This propagator can be expanded in powers of the Coulomb interaction with the leading term giving free propagation

$$\tilde{G}_{\rm NR}(\mathbf{p}_f-\mathbf{k},\mathbf{p}';E_n-k)\cong\frac{-(2\pi)^3\delta^3(\mathbf{p}_f-\mathbf{k}-\mathbf{p})}{(\mathbf{p}_f-\mathbf{k})^2+2mk+\gamma^2}\ . \tag{5.5}$$

If Eq. (5.5) is used in (5.4) we obtain the one-Coulomb (1C) approximation to (5.4). This approximation is not, however, especially useful in the evaluation of (5.4) since the sum over all Coulomb interaction is required. If we use Eq. (5.5) in Eq. (5.4), we can readily identify its contribution in the context of a Feynman diagram approach as

$$(\Delta E_T)_{\rm 1C}=\frac{8(Z\alpha)^2}{(2\pi)^7 M}\int d^3k\,d^3p_i d^3p_f\frac{1}{\mathbf{k}^2(\mathbf{p}_i-\mathbf{p}_f+\mathbf{k})^2}\phi_n^\dagger(\mathbf{p}_f)\times\frac{\mathbf{p}_{f\perp}\cdot(\mathbf{p}_i-\mathbf{p}_f)}{(\mathbf{p}_f-\mathbf{k})^2+2mk+\gamma^2}\phi_n(\mathbf{p}_i)\ . \tag{5.6}$$

It is convenient and more useful, however, to study Eq. (5.3) in more detail by separating it into the terms previously calculated [see separation below Eq. (3.3)]. The first term, obtained by setting $e^{i\mathbf{k}\cdot\mathbf{r}}\to 1$, is called the dipole approximation. It results in

$$(\Delta E_T)_d=\Delta E_{T_1}=\frac{4\pi(Z\alpha)^2}{2\pi^2 mM}\int d^3k\,d^3p_i d^3p_f d^3p'\frac{1}{\mathbf{k}^2(2\pi)^9}\times\phi_n^\dagger(\mathbf{p}_f)\mathbf{p}_{f\perp}\cdot(\mathbf{p}_i-\mathbf{p}')\times 2m\tilde{G}_{\rm NR}(\mathbf{p}_f,\mathbf{p}';E_n-k)\times\frac{1}{(\mathbf{p}_i-\mathbf{p}')^2}\phi_n(\mathbf{p}_i)\ . \tag{5.7}$$

This term was previously calculated and yielded a Bethe logarithm. The presence of the Schrödinger Green's function indicates that Feynman diagrams to arbitrary order in the Coulomb potential are present. Moreover, due to the infrared behavior of the integrals we cannot truncate an expansion of $\tilde{G}_{\rm NR}$ in powers of the Coulomb potential.

Turning next to the correction to the "dipole approximation," we find

$$(\Delta E_T)_{\rm corr}=\Delta E_{T_2}+\Delta E_{T_2'}\ , \tag{5.8}$$

where we can write

$$\Delta E_{T_2}=\frac{Z\alpha}{2\pi^2 mM}\int d^3k\, d^3p_i d^3p_f d^3p'\frac{1}{k^3(2\pi)^9}\left[\phi_n^\dagger(\mathbf{p}_f)\mathbf{p}_{f\perp}\cdot(\mathbf{p}_i-\mathbf{p}')\right.$$
$$\left.\times[(2\pi)^3\delta^3(\mathbf{p}_f-\mathbf{k}-\mathbf{p}')-(2\pi)^3\delta^3(\mathbf{p}_f-\mathbf{p}')]\frac{(-4\pi Z\alpha)}{(\mathbf{p}_i-\mathbf{p}')^2}\phi_n(\mathbf{p}_i)\right], \tag{5.9}$$

$$\Delta E_{T_2'}=\frac{Z\alpha}{2\pi^2 mM}\int d^3k\, d^3p_i d^3p_f d^3p'\frac{1}{k^3(2\pi)^9}\{\phi_n^\dagger(\mathbf{p}_f)\mathbf{p}_{f\perp}\cdot[2m\tilde{G}_{\rm NR}(\mathbf{p}_f-\mathbf{k},\mathbf{p}';E_n-k)$$
$$-2m\tilde{G}_{\rm NR}(\mathbf{p}_f,\mathbf{p}';E_n-k)]\langle\mathbf{p}'|[H,[V,\mathbf{p}]]|\mathbf{p}_i\rangle\phi_n(\mathbf{p}_i)\}\ . \tag{5.10}$$

The first of these becomes

$$\Delta E_{T_2}=\frac{4\pi(Z\alpha)^2}{2\pi^2 mM}\int d^3k\, d^3p_i d^3p_f\frac{1}{k^3(2\pi)^6}\phi_n^\dagger(\mathbf{p}_f)\mathbf{p}_f\cdot(\mathbf{p}_i-\mathbf{p}_f)_\perp\left[\frac{1}{(\mathbf{p}_i-\mathbf{p}_f+\mathbf{k})^2}-\frac{1}{(\mathbf{p}_i-\mathbf{p}_f)^2}\right]\phi_n(\mathbf{p}_i)\ . \tag{5.11}$$

Consider next the correction $\Delta E_{T_2'}$, which leads to (4.22). To evaluate to order $(Z\alpha)^6 m^2/M$ it suffices to keep only the leading terms of $\tilde{G}_{\rm NR}$ and to neglect $E_n$ and $V$ compared to $\mathbf{p}_i^2/2m$ or $\mathbf{p}_f^2/2m$. We then obtain

$$\Delta E_{T_2'}=\frac{4\pi(Z\alpha)^2}{2\pi^2 mM}\int d^3k\, d^3p_i d^3p_f\frac{1}{k^3(2\pi)^6}\phi_n^\dagger(\mathbf{p}_f)\mathbf{p}_{f\perp}\cdot(\mathbf{p}_i-\mathbf{p}_f)$$
$$\times\left[\frac{(\mathbf{p}_f-\mathbf{k})^2-\mathbf{p}_i^2}{(\mathbf{p}_f-\mathbf{k})^2+2mk}\frac{1}{(\mathbf{p}_i-\mathbf{p}_f+\mathbf{k})^2}-\frac{\mathbf{p}_f^2-\mathbf{p}_i^2}{\mathbf{p}_f^2+2mk}\frac{1}{(\mathbf{p}_i-\mathbf{p}_f)^2}\right]\phi_n(\mathbf{p}_i)\ . \tag{5.12}$$

To understand the relation between (5.4) and the Feynman diagrammatic approach discussed in Sec. II, we consider the sets of graphs shown in Figs. 10(a) and 10(b), and follow the procedure of Sapirstein and Yennie. The bracket which spans the interactions on the proton side denotes the sum of all permutations of the interactions, on the proton side, as well as the necessary subtraction of the reducible parts, included in earlier calculations. It should be kept in mind that this does not include all graphs (e.g., permutations of the interactions on the electron side), but as pointed out by Sapirstein and Yennie, those diagrams where the transverse photon does not precede or follow *all* Coulomb photons will be suppressed relative to the leading contribution. Moreover, since the transverse photon already brings in an inverse power of mass $M$, the remaining parts of the diagrams (i.e., propagators) may be treated in the $M\to\infty$ limit. We can then explicitly sum over the permutations, which leads to a simplification in which all loop integrals are three dimensional except for the loop which requires integration over $k$. After this simplification, the effective proton line structure is proportional to $2\mathbf{q}_r/(k_0+i\epsilon)$ for Fig. 10(a) and to $2\mathbf{q}_r/(-k_0+i\epsilon)$ for Fig. 10(b), where $\mathbf{q}_r$ is the momentum carried by the Coulomb interaction "farthest" from the transverse, at the electron side. After this removal we find that our correction to the energy is in complete agreement with the result of Sapirstein and Yennie

$$\Delta E_T=-2\times\frac{1}{M}\sum_{r=1}^{\infty}\int d^3p_f\frac{1}{(2\pi)^3}\phi_n^\dagger(\mathbf{p}_f)\int\prod_{j=1}^{r}d^3p_j\frac{1}{(2\pi)^3}\int d^4k\frac{1}{-(2\pi)^4 i}\frac{(4\pi Z\alpha)}{(-k_0+i\epsilon)(k^2+i\epsilon)}$$
$$\times\left[-\frac{4\pi Z\alpha\gamma_0}{\mathbf{q}_r^2}\prod_{j=1}^{r}\frac{m+p_{i0}\gamma_0+\not{p}_j-\not{k}}{k^2-2p_{i0}k_0-p_j^2+2\mathbf{p}_j\cdot\mathbf{k}-\gamma^2+i\epsilon}\prod_{j=1}^{r-1}\frac{-4\pi Z\alpha\gamma_0}{(\mathbf{p}_j-\mathbf{p}_{j+1})^2}\mathbf{q}_r\cdot\boldsymbol{\gamma}_\perp\right]\phi_n(\mathbf{p}_i) \tag{5.13}$$

$$=-\frac{2}{M}\int d^3p_f\frac{1}{(2\pi)^3}d^3p_i\frac{1}{(2\pi)^3}d^4k\frac{1}{-(2\pi)^4 i}\phi_n^\dagger(\mathbf{p}_f)\frac{4\pi Z\alpha}{(-k_0+i\epsilon)(k^2+i\epsilon)}$$
$$\times\sum_{r=1}^{\infty}\frac{(-4\pi Z\alpha\gamma_0)}{\mathbf{q}_r^2}\left[\int\prod_{j=2}^{r}d^3p_j\frac{1}{(2\pi)^3}\prod_{j=1}^{r}\frac{m+p_{i0}\gamma_0+\not{p}_j-\not{k}}{k^2-2p_{i0}k_0-\mathbf{p}_j^2+2\mathbf{p}_j\cdot\mathbf{k}-\gamma^2+i\epsilon}\prod_{j=1}^{r-1}\frac{-4\pi Z\alpha\gamma_0}{(\mathbf{p}_j-\mathbf{p}_{j+1})^2}\right]$$
$$\times\mathbf{q}_r\cdot\boldsymbol{\gamma}_\perp\phi_n(\mathbf{p}_i)\ , \tag{5.14}$$

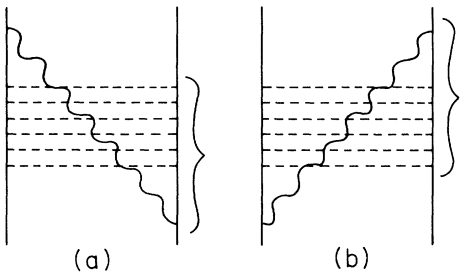


FIG. 10. Transverse exchange with multiple-Coulomb exchange.

where $p_{i0}=m+\epsilon=m-\gamma^2/2m$. The term in large parentheses can be written as

$$S(\mathbf{p}_r-\mathbf{k},\mathbf{p}_i-\mathbf{k};p_{i0}-k_0)\ .$$

It is the Dirac Coulomb propagator. Note that if $r=1$ we simply get the free propagator while subsequent terms in the series give all orders of Coulomb interactions. Equation (5.14) is very similar to the approximate result given by Eq. (5.4), which has already been evaluated, and consequently additional terms are obtained only after an appropriate subtraction has been made.

It is convenient to decompose the electron propagator of (5.14) in terms of projection operators

$$\frac{\not p_j-\not k+m}{(p_j-k)^2-m^2+i\epsilon}=\left[\frac{\Lambda_+(p_j-k)}{p_{j0}-k_0-E(k-p_j)+i\epsilon}+\frac{\Lambda_-(p_j-k)}{p_{j0}-k_0+E(k-p_j)-i\epsilon}\right]\gamma_0$$

and also write

$$\frac{1}{k^2+i\epsilon}=\frac{1}{(k_0-k+i\epsilon)(k_0+k-i\epsilon)}\ .$$

We will carry out the $k_0$ integrations of (5.14) by closing the contour in the lower half-plane. Poles will be located at $k_0=k$ or at $k_0=p_{j0}+E(k-p_j)$, the former being the more dominant contribution. Consider first the contribution from the photon pole together with all the positive-energy projection terms. In the nonrelativistic limit, we find

$$-\frac{2}{M}\int d^3p_f d^3p_i d^3k\frac{1}{(2\pi)^9}\tilde\phi_n^\dagger(\mathbf{p}_f)\frac{(-4\pi Z\alpha)}{2\mathbf{k}^2}\times\sum_{r=1}^{\infty}\frac{(-4\pi Z\alpha)}{\mathbf{q}_r^2}\left[\int\prod_{j=2}^{r}d^3p_j\frac{1}{(2\pi)^3}\prod_{j=1}^{r-1}\frac{(-4\pi Z\alpha)}{(\mathbf{p}_j-\mathbf{p}_{j+1})^2}\prod_{j=1}^{r}\frac{1}{p_{j0}-k-E(k-p_j)}\mathbf{q}_{r\perp}\cdot\frac{\mathbf{p}_i}{m}\tilde\phi_n(\mathbf{p}_i)\right],\quad(5.15)$$

where $\tilde\phi$ is the nonrelativistic wave function. Approximating $E(k-p_j)$ by its nonrelativistic expression, we obtain

$$-\sum_{r=1}^{\infty}\frac{1}{mM}\int d^3p_f d^3p_i d^3k\frac{1}{(2\pi)^9}\tilde\phi_n^\dagger(\mathbf{p}_f)\left[\frac{-4\pi Z\alpha}{(\mathbf{p}_r-\mathbf{k}-\mathbf{p}_f)^2}\right]\left[\frac{-4\pi Z\alpha}{\mathbf{k}^2}\right]\times\prod_{j=2}^{r}d^3p_j\frac{1}{(2\pi)^3}\left[\prod_{j=1}^{r}\frac{(-2m)^r}{2mk+\gamma^2+(\mathbf{p}_j-\mathbf{k})^2}\prod_{j=1}^{r-1}\frac{(-4\pi Z\alpha)}{(\mathbf{p}_j-\mathbf{p}_{j+1})^2}(\mathbf{p}_r-\mathbf{p}_f)_\perp\cdot\mathbf{p}_i\right]\tilde\phi_n(\mathbf{p}_i)\ .\quad(5.16)$$

At this point we will define $\mathbf{p}'=\mathbf{p}_r$ for whatever value $r$ might have in the sum. This allows us to rewrite (5.16) as

$$\frac{1}{mM}\int d^3p_f d^3p_i d^3k d^3p'\frac{1}{(2\pi)^{12}}\tilde\phi_n^\dagger(\mathbf{p}_f)\frac{(-4\pi Z\alpha)}{(\mathbf{p}'-\mathbf{k}-\mathbf{p}_f)^2}\frac{(-4\pi Z\alpha)}{\mathbf{k}^2}\times\left[\sum_{r=1}^{\infty}\prod_{j=2}^{r-1}d^3p_j\frac{1}{(2\pi)^3}\left[\prod_{j=1}^{r}\frac{(-2m)^r}{2mk+\gamma^2+(\mathbf{p}_j-\mathbf{k})^2}\prod_{j=1}^{r-1}\frac{(-4\pi Z\alpha)}{(\mathbf{p}_j-\mathbf{p}_{j+1})^2}\right]\right](\mathbf{p}_f-\mathbf{p}')_\perp\cdot\mathbf{p}_i\tilde\phi_n(\mathbf{p}_i)\ .\quad(5.17)$$

The expression in square brackets contains $\mathbf{p}'-\mathbf{k}$ as well as $\mathbf{p}_1-\mathbf{k}$ (same as $\mathbf{p}_i-\mathbf{k}$). This expression is exactly the nonrelativistic Green's function we encountered earlier in Eq. (5.4) except for a difference of variables. The above expression is

$$\frac{2(Z\alpha)^2}{\pi mM}\int d^3p_f d^3p_i d^3k\ d^3p'\frac{1}{(2\pi)^9\mathbf{k}^2}\tilde\phi_n^\dagger(\mathbf{p}_f)\frac{(\mathbf{p}_f-\mathbf{p}')\cdot\mathbf{p}_{i\perp}}{(\mathbf{p}'-\mathbf{k}-\mathbf{p}_f)^2}\times 2m\tilde G_{\rm NR}(\mathbf{p}'-\mathbf{k},\mathbf{p}_i-\mathbf{k};E_n-k)\tilde\phi_n(\mathbf{p}_i)\ ,\quad(5.18)$$

which corresponds to Fig. 10(b) while Eq. (5.4) corresponds to Fig. 10(a). We have stated previously that these contributions to the energy shift are equal and have incorporated a factor of 2 to account for this.

### C. Single-Coulomb–single-transverse calculation

The problem we now face is to extract from Eq. (5.14) new contributions beyond Eq. (5.18). Since this latter expression is easily identified within the former, the process of calculating new contributions is relatively straightfor-

ward. To begin, we look at terms which have a single loop, namely the $r=1$ term of Eq. (5.14) (see Fig. 11). The $k_0$ contour integral is closed below the axis and contributions arise from the photon pole and from the electron pole, with the photon pole being dominant. The electron propagator can be decomposed into positive- and negative-energy projection operators. The former contains the corresponding portion of (5.18), while the latter is a new contribution which, in the language of time-ordered perturbation theory, comes from the so-called $Z$ graph.

Let $\Delta E_{C\text{-}T}$ be the single-loop contribution to (5.14). It may be written as

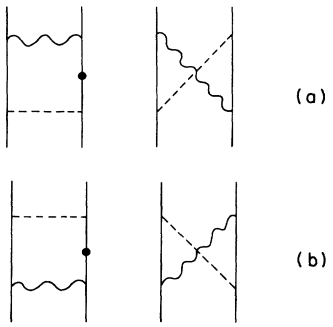


FIG. 11. Single-Coulomb–single-transverse graphs.

$$\Delta E_{C\text{-}T}=\frac{8(Z\alpha)^2}{(2\pi)^7 M}\int d^3k\, d^3p_i d^3p_f \frac{1}{2E_{p_i-k}(\mathbf{p}_i-\mathbf{p}_f-\mathbf{k})^2}\phi^\dagger(p_f) \times\left[\frac{E_{p_i-k}+\boldsymbol{\alpha}\cdot(\mathbf{p}_i-\mathbf{k})+\beta m}{2\mathbf{k}^2(k-p_{i0}+E_{p_i-k})}+\frac{E_{p_i-k}-\boldsymbol{\alpha}\cdot(\mathbf{p}_i-\mathbf{k})-\beta m}{2\mathbf{k}^2(k-p_{i0}-E_{p_i-k})}\left[1-\frac{2\mathbf{k}^2}{(p_{i0}+E_{p_i-k})(p_{i0}+E_{p_i-k}+k)}\right]\right] \times\boldsymbol{\alpha}_\perp\cdot(\mathbf{p}_i-\mathbf{p}_f)\phi(p_i) \tag{5.19}$$

and let $\Delta E_+$ be the single-loop contribution to (5.18), namely

$$\Delta E_+=\frac{8(Z\alpha)^2}{(2\pi)^7 M}\int d^3k\, d^3p_i d^3p_f \frac{1}{\mathbf{k}^2(\mathbf{p}_i-\mathbf{p}_f-\mathbf{k})^2}\tilde{\phi}^\dagger(p_f) \times\frac{\mathbf{p}_{i\perp}\cdot(\mathbf{p}_i-\mathbf{p}_f)}{2mk+\gamma^2+(\mathbf{p}_i-\mathbf{k})^2}\tilde{\phi}(p_i)\ . \tag{5.20}$$

We need to compute the difference

$$\Delta E_{C\text{-}T}-\Delta E_+\ .$$

For the wave function $\phi(\mathbf{p})$, we use

$$\phi(\mathbf{p})\cong\begin{bmatrix}\chi\\ \dfrac{\boldsymbol{\sigma}\cdot\mathbf{p}\chi}{2m}\end{bmatrix}\tilde{\phi}(\mathbf{p})\ ,$$

where $\chi$ is a two-component electron spinor, and $\tilde{\phi}(\mathbf{p})$ is again the nonrelativistic momentum space wave function. The lower component of this wave function has the proper asymptotic behavior. We can use a "better" wave function (i.e., one obtained by iterating the above wave function in the momentum space Dirac equation), but this is unnecessary, as our results are not sensitive to these corrections. It is convenient to choose the following angles:

$$\mathbf{p}_i\cdot\mathbf{k}=p_i k\cos\theta_i\ ,$$

$$\mathbf{p}_f\cdot\mathbf{k}=p_f k\cos\theta_f\ ,$$

$$\mathbf{p}_i\cdot\mathbf{p}_f=p_i p_f[\cos\theta_i\cos\theta_f+\sin\theta_i\sin\theta_f\cos(\phi_i-\phi_f)]\ .$$

As there are no other angles in the problem, the $d\Omega_k$ integral is trivially $4\pi$. For $2S$ and $2P$ wave functions we use

$$\tilde{\phi}_{2S,\pm1/2}(\mathbf{p})=32\pi\gamma^{5/2}\frac{p^2-\gamma^2}{(p^2+\gamma^2)^3}Y_{00}(\theta,\phi)|\pm\rangle\ ,$$

$$\tilde{\phi}_{2P,1/2}(\mathbf{p})=[-\sqrt{1/3}Y_{10}(\theta,\phi)|+\rangle +\sqrt{2/3}Y_{11}(\theta,\phi)|-\rangle]\tilde{\phi}_{2P}(p)\ ,$$

$$\tilde{\phi}_{2P,-1/2}(\mathbf{p})=[-\sqrt{2/3}Y_{1-1}(\theta,\phi)|+\rangle +\sqrt{1/3}Y_{10}(\theta,\phi)|-\rangle]\tilde{\phi}_{2P}(p)\ ,$$

where

$$\tilde{\phi}_{2P}(p)=-64\pi i\left[\frac{\gamma^3}{3}\right]^{1/2}\frac{\gamma^2 p}{(p^2+\gamma^2)^3}\ .$$

These wave functions are normalized by

$$\int d^3p\frac{1}{(2\pi)^3}\tilde{\phi}^\dagger(\mathbf{p})\tilde{\phi}(\mathbf{p})=1\ .$$

Since the result will be independent of the $m_J$ quantum number we use the average of the $m_J=+\frac{1}{2}$ and $-\frac{1}{2}$ $P$-state wave functions, which are purely imaginary. We are then left with a seven-dimensional integral which we carry out using VEGAS.

The overall result for hydrogen with $n=2$, which is almost entirely from the $S$ state, is

$$\Delta E_{C\text{-}T}-\Delta E_+=8.023\pm0.027\ \text{kHz}\ . \tag{5.21}$$

where the error is given by VEGAS. The bulk of this correction ($10.805\pm0.034$ kHz) is due to the entire $Z$

graph or negative-energy term while the remainder is due to the positive-energy part minus $\Delta E_+$. Due to the complicated nature of the integrand, we have not been able to fully extract an analytical result. We have, however, found that there is a large logarithmic contribution of $2[(Z\alpha)^6 \ln(1/Z\alpha)]m^2/M$.

We have also performed the calculation without decomposing the electron propagator into positive- and negative-energy projection operators. In place of Eq. (5.19), we now have

$$\Delta E_{C\text{-}T}=\frac{8(Z\alpha)^2}{(2\pi)^7 M}\int d^3k\, d^3p_i d^3p_f \frac{1}{(\mathbf{p}_i-\mathbf{p}_f-\mathbf{k})^2}\phi^\dagger(\mathbf{p}_f)\left[\frac{\not p_i - k\gamma_0+\boldsymbol{\gamma}\cdot\mathbf{k}+m}{2\mathbf{k}^2(2kp_{i0}+(\mathbf{p}_i-\mathbf{k})^2-\mathbf{k}^2+m^2-p_{i0}^2)} - \frac{\not p_i-(E_{p_i-k}+p_{i0})\gamma_0+\boldsymbol{\gamma}\cdot\mathbf{k}+m}{2E_{p_i-k}(p_{i0}+E_{p_i-k})[(p_{i0}+E_{p_i-k})^2-\mathbf{k}^2]}\right] \times \boldsymbol{\gamma}_\perp\cdot(\mathbf{p}_i-\mathbf{p}_f)\phi(\mathbf{p}_i)\ , \tag{5.22}$$

where the first term in the large parentheses is the photon pole term, and the second term is the electron pole term. After performing the necessary Dirac algebra, we are left with terms proportional to

$$\mathbf{p}_i\cdot(\mathbf{p}_i-\mathbf{p}_f)_\perp\ ,$$

$$(1/2m)(\mathbf{p}_i+\mathbf{p}_f)\cdot(\mathbf{p}_i-\mathbf{p}_f)_\perp\ ,$$

and

$$(1/4m^2)[\mathbf{p}_f\cdot(2\mathbf{p}_i-\mathbf{k})\mathbf{p}_i\cdot(\mathbf{p}_i-\mathbf{p}_f)_\perp - \mathbf{p}_i\cdot(\mathbf{p}_i-\mathbf{k})\mathbf{p}_f\cdot(\mathbf{p}_i-\mathbf{p}_f)_\perp]\ ;$$

each of these terms has a photon pole contribution and an electron pole contribution. The subtraction of $\Delta E_+$ [Eq. (5.20)] can be performed analytically, by combining it with the $\mathbf{p}_i\cdot(\mathbf{p}_i-\mathbf{p}_f)_\perp$ term derived from (5.19). The grouping together of photon and electron pole contributions facilities the integration of (5.22) with VEGAS, by adding convergence in the high-$k$ limit (as $k$ approaches infinity, the coefficients of the three terms above separately vanish). This second approach has the benefit that after subtraction of $\Delta E_+$ the leading term $\mathbf{p}_i\cdot(\mathbf{p}_i-\mathbf{p}_f)$, photon pole part, has a simpler form and therefore can be partially calculated analytically to a greater extent. The straightforward numerical approach of using VEGAS to calculate $\Delta E_{C\text{-}T}-\Delta E_+$ yields identical results (within errors) whether we use (5.19) or (5.22) for $\Delta E_{C\text{-}T}$. Of course this is expected, but it is nevertheless comforting to see the same result emerge by organizing the calculation in several different ways.

We have also found that leading approximations to (5.22) produce a very simple result. We find that

$$\Delta E_{C\text{-}T}-\Delta E_+ \cong \frac{8(Z\alpha)^2}{(2\pi)^7 M} \times\int d^3k\, d^3p_i d^3p_f \frac{1}{(\mathbf{p}_i-\mathbf{p}_f-\mathbf{k})^2}\tilde\phi^\dagger(\mathbf{p}_f) \times\frac{\mathbf{p}_{i\perp}\cdot\mathbf{p}_i}{[2mk+\gamma^2+(\mathbf{p}_i-\mathbf{k})^2]^2}\tilde\phi(\mathbf{p}_i)\ .$$

To arrive at this we retain only the leading term in the numerator and we also make use of the electron pole contribution to the negative-energy term. This is needed to cancel a pole at $k=p_{i0}+E_{p_i-k}$ and to convert a denominator factor $2mk+\gamma^2+(\mathbf{p}_i-\mathbf{k})^2-\mathbf{k}^2$ to $2mk+\gamma^2+(\mathbf{p}_i-\mathbf{k})^2$. The integral over momentum $\mathbf{p}_f$ can now be carried out using the Schrödinger equation to obtain the expression

$$\frac{2Z\alpha}{(2\pi)^5 mM}\int d^3k\, d^3p_i \mathbf{p}_{i\perp}\cdot\mathbf{p}_i[(\mathbf{p}_i-\mathbf{k})^2+\gamma^2] \times\frac{\tilde\phi^\dagger(\mathbf{p}_i-\mathbf{k})\tilde\phi(\mathbf{p}_i)}{[2mk+\gamma^2+(\mathbf{p}_i-\mathbf{k})^2]^2}\ ,$$

which easily produces a three-dimensional integral. When this is integrated numerically it produces nearly the same result as (5.21); the difference is presumably due to relativistic corrections.

### D. Double-Coulomb–single-transverse calculation

Now we consider the contribution from two loops. This corresponds to a sum of 18 diagrams shown in Fig. 12. A number of diagrams shown in Fig. 12 are con-

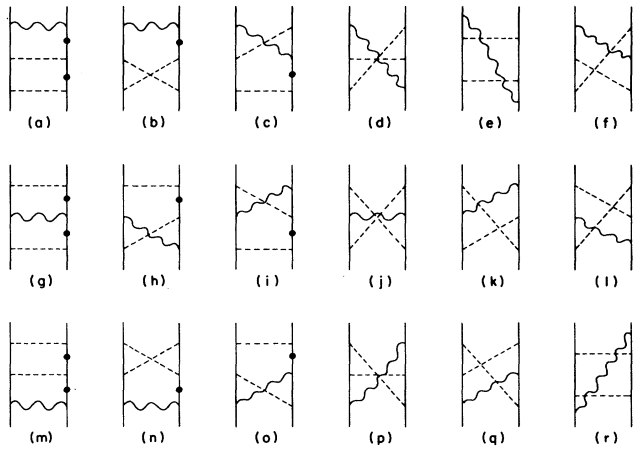


FIG. 12. Double-Coulomb–single-transverse graphs.

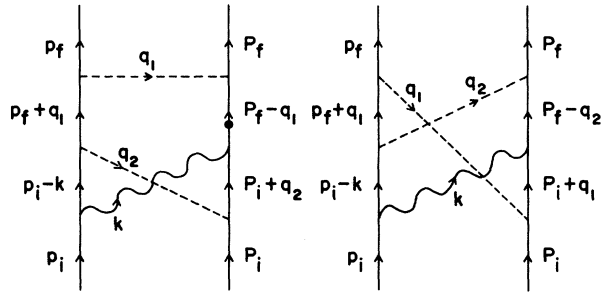


FIG. 13. Contributing double-Coulomb–single-transverse graphs.

tained in Eq. (5.13), namely the graphs in which the transverse photon on the electron side precedes or follows all Coulomb interactions. According to Sapirstein and Yennie,[6] the diagrams with electron line structure of Coulomb-transverse-Coulomb do not contribute to leading order. After performing the subtractions as indicated by the dots on the proton line, as well as the subtraction which removes the two-loop contribution to Eq. (5.18), which has already been calculated in old-fashioned perturbation theory, we expect these diagrams to contribute to $O((Z\alpha)^6 m^2/M)$. It is sufficient, then, to set external momenta to zero, as keeping external momenta will give corrections to the zero-momentum contribution that are higher order in $Z\alpha$. Figures 12(a), 12(b), 12(d), 12(f), 12(h), 12(i), 12(k), 12(l), 12(m), 12(n), 12(p), and 12(r) will lead to an integrand proportional to external momenta or to $\gamma_\perp \cdot \mathbf{k}$ (which is identically zero). Thus, at our level of approximation we can ignore these contributions. Figures 12(g) and 12(j) can be readily shown to cancel each other. We are thus in agreement with Sapirstein and Yennie, in that the diagrams with electron line structure Coulomb-transverse-Coulomb will not contribute to leading order. Of the remaining four diagrams, we will calculate those in Figs. 12(o) and 12(q), and simply double the result to pick up the contribution from Figs. 12(c) and 12(f). We label the momenta as shown in Fig. 13. We chose to calculate this contribution explicitly, instead of using the $r=2$ part of Eq. (5.14), in order to discover which diagrams are the most significant. It is straightforward to show that (5.24) below does indeed reproduce the $r=2$ part of (5.14).

The proton line structure is found to be

$$P_i = \frac{i(Ze)^3}{2M}\frac{(q_1-q_2)_i}{q_{10}+i\epsilon}(-2\pi i)\delta(q_{20}) . \tag{5.23}$$

The total energy shift $\Delta E_{\text{dC-}T}$ is found to be

$$\Delta E_{\text{dC-}T} = 2i\int d^4k\, d^4q_1 d^4q_2 d^3p_i d^3p_f \frac{\tilde{\phi}^\dagger(p_f)}{(2\pi)^{18}}\left[\frac{-ig^{ij}}{k^2+i\epsilon}\frac{i}{\mathbf{q}_1^2}\frac{i}{\mathbf{q}_2^2}\right]\left[\frac{i(Ze)^3}{2M}\frac{(q_1-q_2)_i}{q_{10}+i\epsilon}(-2\pi i)\delta(q_{20})\right]$$
$$\times(2\pi)^4\delta^4(k+q_1+q_2)\left[\bar{u}(p_f)(-ie\gamma_0)\frac{i}{\not p_f+\not q_1-m+i\epsilon}(-ie\gamma_0)\frac{i}{\not p_i-\not k-m+i\epsilon}\right.$$
$$\left.\times(-ie\gamma_\perp)_j u(p_i)\right]\tilde{\phi}(p_i)-\cdots , \tag{5.24}$$

where the ellipses represent a two-loop contribution to (5.18). We can integrate over $q_2$, using the $\delta$ function, and also over $q_{10}$. We can also decompose the electron propagators into positive-energy and negative-energy parts, and perform the necessary Dirac algebra. Using the approximation

$$u(p)\simeq\begin{bmatrix}\chi\\0\end{bmatrix},$$

and the fact that we have ignored external momenta in the kernel, we can also integrate over $p_i$ and $p_f$. Then

$$\Delta E_{\text{dC-}T} = \frac{4i(Z\alpha)^3|\psi(0)|^2}{(2\pi)^4 M}$$
$$\times\int d^4k\, d^3q \frac{\mathbf{q}_\perp\cdot\mathbf{q}}{\mathbf{q}^2(\mathbf{q}+\mathbf{k})^2E_qE_k}\frac{1}{(k_0-k+i\epsilon)(k_0+k-i\epsilon)(k_0-i\epsilon)}$$
$$\times\left[\frac{(E_k-m)}{(k_0-m+E_q-i\epsilon)(k_0-m+E_k-i\epsilon)}+\frac{(E_k+m)}{(k_0-m+E_q-i\epsilon)(k_0-m-E_k+i\epsilon)}\right.$$
$$\left.-\frac{(E_k-m)}{(k_0-m-E_q+i\epsilon)(k_0-m+E_k-i\epsilon)}-\frac{(E_k+m)}{(k_0-m-E_q+i\epsilon)(k_0-m-E_k+i\epsilon)}\right] . \tag{5.25}$$

Finally, we can perform the $k_0$ integral by closing the contour in the upper half-plane, and after much algebraic simplification,

$$\Delta E_{\mathrm{dC}\text{-}T}=\frac{-4(Z\alpha)^3|\psi(0)|^2}{(2\pi)^3 M}\times\int d^3k\,d^3q\frac{\mathbf{q}_\perp\cdot\mathbf{q}}{E_qE_k\mathbf{q}^2(\mathbf{q}+\mathbf{k})^2}\left[\frac{E_kE_q}{mk^2[2mk+(\mathbf{q}^2-\mathbf{k}^2)]}-\left[\frac{2m^2}{E_q+E_k}+(2m+E_q)\right]\frac{1}{m(m+E_k)[2m(m+E_q)+\mathbf{q}^2-\mathbf{k}^2)]}\right]. \tag{5.26}$$

Three of the angular integrals are trivial, and the remaining three dimensional integral can be easily performed using VEGAS. The result is a $(Z\alpha)^6m^2/M$ contribution of

$$\Delta E_{\mathrm{dC}\text{-}T}=-1.904\pm0.001\ \mathrm{kHz}\ . \tag{5.27}$$

Adding (5.21) to (5.27) we find a new total correction of 6.1 kHz.

## VI. CONCLUSION AND SUMMARY OF THE LAMB SHIFT

We have now completed the pure recoil corrections to the hydrogen Lamb shift through order $(Z\alpha)^6m^2/M$. Let us denote the various contributions by $\Delta E_{1\mathrm{C}}$ (double Coulomb), $\Delta E_{t\mathrm{C}}$ (triple Coulomb), $\Delta E_{\mathrm{dT}}$ (double transverse), $\Delta E_{\mathrm{dT\text{-}1C}}$ (double-transverse–single-Coulomb), $\Delta E_{s\mathrm{C}}$ (analytically calculated part of single transverse), and $\Delta E_{\Delta s\mathrm{T}}$ (new corrections to single transverse). These are now given as follows:

$$\Delta E_{\mathrm{dC}}=-\frac{4(Z\alpha)^2|\psi(0)|^2}{3mM}\left[1-\frac{3\pi Z\alpha}{8}\right], \tag{6.1a}$$

$$\Delta E_{t\mathrm{C}}=-\frac{4(Z\alpha)^2|\psi(0)|^2}{3mM}\left[-\frac{3\pi Z\alpha}{8}\right], \tag{6.1b}$$

$$\Delta E_{\mathrm{dT}}=-\frac{4(Z\alpha)^2|\psi(0)|^2}{3mM}\times\left[-\tfrac{3}{2}(\ln Z\alpha+\tfrac{7}{4})-2(1-\ln2)+\frac{3\pi}{4}Z\alpha\ln\left[\frac{2}{Z\alpha}\right]+\frac{9\pi Z\alpha}{8}\right], \tag{6.1c}$$

$$\Delta E_{\mathrm{dT\text{-}1C}}=\Delta E_{s\mathrm{C}}=-\frac{4(Z\alpha)^3|\psi(0)|^2}{3mM}(-1.81\pm0.001)\ , \tag{6.1d}$$

$$\Delta E_{s\mathrm{T}}=-\frac{4(Z\alpha)^3|\psi(0)|^2}{3mM}\times\left[-2\ln\left[\frac{mZ\alpha}{\Delta E}\right]-\frac{25}{6}-\frac{9\pi Z\alpha}{4}\right], \tag{6.1e}$$

$$\Delta E_{\Delta s\mathrm{T}}=-\frac{4(Z\alpha)^3|\psi(0)|^2}{3mM}\times\left[-\frac{3\pi}{2}\ln\left[\frac{1}{Z\alpha}\right]+8.30\pm0.05+3.53\pm0.001\right], \tag{6.1f}$$

where the last expression comes from single-Coulomb and double-Coulomb corrections to the expression 6.1(e). The sum of these pure recoil terms is

$$\Delta E_{\mathrm{recoil}}=\frac{4(Z\alpha)^2}{3mM}|\psi(0)|^2\left[-1+\tfrac{3}{4}\pi Z\alpha+2\ln(mZ\alpha/\Delta E)+\tfrac{25}{6}+\tfrac{9}{4}\pi Z\alpha+\tfrac{3}{2}(\ln Z\alpha+\tfrac{7}{4})+2(1-\ln2)-\tfrac{3}{4}\pi Z\alpha\ln(2/Z\alpha)-\tfrac{9}{8}\pi Z\alpha+\left[1.81+\frac{3\pi}{2}\ln(1/Z\alpha)-8.30-3.53\right]Z\alpha\right]. \tag{6.2}$$

Thus the $(Z\alpha)^6m^2/M$ contribution is

$$[(Z\alpha)^6m^2/n^3M][\tfrac{5}{2}-\ln(2/Z\alpha)+2\ln(1/Z\alpha)-4.25]\ , \tag{6.3}$$

which gives +3.15 kHz for the $n=2$ state of hydrogen. Thus the new corrections to the single-transverse contribution, which are predominantly from the negative-energy (or $Z$-graph) terms of single-transverse–single-Coulomb interactions are large. This was a surprise to us and is presumably due to the logarithmic character of this contribution, as mentioned earlier.

The net result is to substantially increase the Lamb-shift results to

$$\delta E_{\mathrm{Lamb}}=1\,057\,855(11)\ \mathrm{kHz}\ \text{ if } r_p=0.805(11)\ \mathrm{fm}$$
$$=1\,057\,873(11)\ \mathrm{kHz}\ \text{ if } r_p=0.862(12)\ \mathrm{fm}\ . \tag{6.4}$$

If there were no further corrections these results would favor the smaller radius when compared with the experimental results of 1 057 845(9) kHz (Lundeen and Pipkin[7]) and 1 057 851(2) kHz (Pal'chikov, Sokolov, and Yakovlev[8]). However, as stressed earlier, there are still two-loop nonrecoil binding corrections which must still be calculated. Therefore conclusions drawn from a comparison of current theory and experiment are premature.

For completeness, we provide the current theoretical

expression for the Lamb shift. It is obtained from Eq. (8) of Ref. 4. In that equation we alter the $(Z\alpha)^6 m^2/M$ by replacing 3 by $\frac{5}{2}$ thus correcting an error previously noted in an erratum,[4] and we replace previously unknown terms denoted by $+\cdots$ by $2\ln(1/Z\alpha)-4.25$, as indicated in Eq. (6.3) above. To obtain this we extracted the logarithmic dependence analytically and determined the remainder numerically. To check the $Z\alpha$ dependence we also verified the correctness of this expression by numerical calculations for various values of $Z\alpha$. The expression now obtained is

$$\begin{aligned}\Delta E_{\text{Lamb}} &= \Delta E_{2S_{1/2}} - \Delta E_{2P_{1/2}} \\ &= [\alpha(Z\alpha)^4 m/6\pi](\mu/m)^3\{\tfrac{1}{8}m/\mu + \ln(Z\alpha)^{-2} - 2.207\,909 + \pi Z\alpha(\tfrac{427}{128} - \tfrac{3}{2}\ln 2) \\ &\quad + (Z\alpha)^2[-\tfrac{3}{4}\ln^2(Z\alpha)^{-2} + (4\ln 2 + \tfrac{55}{48})\ln(Z\alpha)^{-2}] \\ &\quad + (Z\alpha)^2[G_{\text{SE}}(Z\alpha) + G_{\text{VP}}(Z\alpha)] + \alpha(0.323/\pi)\} \\ &\quad + [(Z\alpha)^5 m^2/6\pi M]\{\tfrac{1}{4}\ln(Z\alpha)^{-2} + 2.399\,77 + \tfrac{3}{4}\pi Z\alpha[\tfrac{5}{2} + \ln(1/2Z\alpha) - 4.25]\} + \tfrac{1}{12}(Z\alpha)^4 m^3\langle r_p^2\rangle \\ &\quad - \tfrac{1}{48}[m^3(Z\alpha)^4/M^2] + [\alpha(Z\alpha)^5 m^2/8M][(\tfrac{35}{4}\ln 2 - \tfrac{39}{5} + \tfrac{31}{192}) + (-0.415 \pm 0.004)] \,. \end{aligned} \tag{6.5}$$

The terms $G_{\text{SE}}$ and $G_{\text{VP}}$ denote self-energy and vacuum polarization contributions which for hydrogen ($Z=1$) sum to $-24.0\pm 1.2$. For $Z\neq 1$ the reader is referred to Ref. 9. The above expression does not contain the unknown $\alpha^2(Z\alpha)^5 m$ corrections which are currently under investigation and which are necessary to complete the Lamb shift calculation to the desired accuracy.

## ACKNOWLEDGMENTS

We are indebted to D. R. Yennie and J. R. Sapirstein for pointing out to us the potential importance of negative-energy state contributions in single-transverse exchange. We greatly appreciate the comments of D. R. Yennie, who read and critiqued an early version of this paper. The support of National Science Foundation under Grant No. PHY-8819727-01 is gratefully acknowledged.

[1] J. L. Gorelick and H. Grotch, J. Phys. G **3**, 751 (1977).
[2] H. Grotch and D. R. Yennie, Z. Phys. **202**, 425 (1967); Rev. Mod. Phys. **41**, 350 (1969).
[3] E. E. Salpeter, Phys. Rev. **87**, 328 (1952); T. Fulton and P. C. Martin, *ibid.* **95**, 811 (1954).
[4] G. W. Erickson and H. Grotch, Phys. Rev. Lett. **60**, 2611 (1988); **63**, 1326(E) (1989).
[5] M. A. Doncheski, H. Grotch, and D. A. Owen, Phys. Rev. A **41**, 2851 (1990).
[6] J. Sapirstein and D. R. Yennie, in *Quantum Electrodynamics*, edited by T. Kinoshita (World, Scientific, Singapore, 1990).
[7] S. R. Lundeen and F. M. Pipkin, Phys. Rev. Lett. **46**, 232 (1981); Metrologia **22**, 9 (1986).
[8] V. G. Pal'chickov, Yu. L. Sokolov, and V. P. Yakovlev, Pis'ma Zh. Eksp. Teor. Fiz. **38**, 347 (1983) [JETP Lett. **38**, 418 (1983)].
[9] P. J. Mohr, Phys. Rev. Lett. **34**, 1050 (1975).